



*A Preliminary Comparison
of Mineral Deposits in Faults
near Yucca Mountain, Nevada,
with Possible Analogs*

HYDROLOGY DOCUMENT NUMBER 515

Los Alamos

*Los Alamos National Laboratory is operated by the University of California for
the United States Department of Energy under contract W-7405-ENG-36.*

Prepared by Nevada Nuclear Waste Storage Investigations (NNWSI) Project participants as part of the Civilian Radioactive Waste Management Program. The NNWSI Project is managed by the Waste Management Project Office of the US Department of Energy, Nevada Operations Office. NNWSI Project work is sponsored by the Office of Geologic Repositories of the DOE Office of Civilian Radioactive Waste Management.

An Affirmative Action/Equal Opportunity Employer

This report was prepared as an account of work sponsored by an agency of the United States Government. Neither the United States Government nor any agency thereof, nor any of their employees, makes any warranty, express or implied, or assumes any legal liability or responsibility for the accuracy, completeness, or usefulness of any information, apparatus, product, or process disclosed, or represents that its use would not infringe privately owned rights. Reference herein to any specific commercial product, process, or service by trade name, trademark, manufacturer, or otherwise, does not necessarily constitute or imply its endorsement, recommendation, or favoring by the United States Government or any agency thereof. The views and opinions of authors expressed herein do not necessarily state or reflect those of the United States Government or any agency thereof.

*A Preliminary Comparison
of Mineral Deposits in Faults
near Yucca Mountain, Nevada,
with Possible Analogs*

D. T. Vaniman

D. L. Bish

S. Chipera

CONTENTS

ABSTRACT	1
I. INTRODUCTION	1
II. ANALYTICAL METHODS	7
III. RESULTS	7
IV. DISCUSSION	11
A. Deposits Within Faults Near Yucca Mountain	13
1. Samples from Trench 14	14
Sample T14-F	14
Sample T14-11	20
Sample T14-10	20
Drusy Quartz in Trench 14	23
2. Sample from Trench 17	24
B. Hydrothermal Vein Deposits Near Yucca Mountain	26
C. Warm-Spring Deposits	27
1. Spring Deposits in Oasis Valley	27
2. Warm-Spring Sinter Deposits	28
3. The Paleospring Mound at Wahmonie	30
D. Cold Springs or Seeps, and Playa Deposits	30
1. Paleospring Deposits South of Yucca Mountain?	34
2. Paleospring Deposit Near Moapa	34
3. Playa and Playa/Seep Deposits of the Amargosa Valley	37
E. Soil Deposits	37
F. Calcite-Silica Deposits in Aeolian Sequences	39
V. SUMMARY AND CONCLUSIONS	46
REFERENCES	51

TABLES

TABLE I.	PREPARATION PROCEDURES USED FOR SAMPLES DESCRIBED IN THE TEXT	8
TABLE II.	X-RAY DIFFRACTION DATA	10
TABLE III.	PETROGRAPHIC DATA	12
TABLE IV.	ELECTRON MICROPROBE ANALYSES OF CALCITES	13

FIGURES

1A.	Locations of some warm springs (dots) and of warm-spring sinter deposits (triangles) in northern Nevada. The inset rectangle shows the area detailed in Fig. 1B	2
1B.	Sample localities mentioned in the text, other than those in northern Nevada (Fig. 1A) and near Yucca Mountain (Fig. 1C)	3
1C.	Sample localities near Yucca Mountain	4
2.	Photograph of the southern wall of Trench 14 with sample localities mentioned in the text. The notebook placed on the wall of the trench is 21 cm (8.5 in.) long	5
3.	Photomicrograph of sample T14-F. The clear band of opal-A (sample split T14-FA) overlies earlier layers of calcite with opal-CT (sample split T14-FB)	15
4.	XRD patterns of T14-FA and T14-FB compared. The peaks labeled are calcite (C), opal-A (O-A), Quartz (Q), and clay (CL). The inset photomicrograph shows remnant organic structure within the opal-A of T14-FA; all structures shown consist of opal	16
5.	Comparative XRD patterns of opal-A, opal-CT, and opal-C	17
6.	XRD pattern of sepiolite (S) in the <2- μ m-size fraction of sample T14-FB	18
7.	A map of chain-structure clay (sepiolite) distributions in soils, faults, and a spring seep around Yucca Mountain (after Jones 1983). The locality of Trench 14 and of sand ramps south of the trench is also shown	19
8.	XRD patterns comparing the calcite (C) and opal-CT (O-CT) of a dense calcite-silica band (T14-11 brown) and its outer coating of laminated botryoidal opal-CT (T14-11 white)	21

9.	XRD patterns comparing the fault deposit (T14-10 vein) and the adjacent matrix of the altered tuff (T14-10 gdms) at a locality within the altered Tiva Canyon member in Trench 14 (Fig. 2). The minerals shown are calcite (C), opal-CT (O-CT), quartz (Q), and clay (CL). Inset photomicrographs show representative textures of the two samples. The photomicrograph of T14-10 vein shows both colloform and coarse birefringent opal. The photomicrograph of T14-10 gdms shows calcite crystals (C) and late opal (O-CT).	22
10.	XRD patterns of both a bulk sample (TR-17) and an acid-treated sample (TR17-1 acid residue) from Trench 17. Inset photomicrograph shows possible relic ooids(?) within the bulk sample. The diffraction peaks of calcite (C), opal-CT (O-CT), quartz (Q), and clay (CL) are labeled . . .	25
11.	XRD pattern of a hydrothermal vein from the Calico Hills. The minerals labeled are quartz (Q), opal-C (O-C), and cryptomelane (Cr)	28
12.	XRD pattern of spring efflorescence from Oasis Valley. The diffraction peaks labeled are halite (H), burkeite (B), and trona (T)	29
13.	XRD patterns of opal-A sinter from the warm springs at Brady (RMV-201-82) and at Steamboat Hot Springs (RMV-205-D). Inset photomicrograph shows tubules of organic origin containing small pyrite crystals in the opal-A of sample RMV-205-D	31
14.	Gypsum (G) of the paleospring deposit near Wahmonie, with minor amounts of calcite (C) and clay (CL)	32
15.	Calcite (C) of the dense microspar tufa from Nevares. Inset photomicrograph shows scalenohedral habit of the calcite microspar	33
16.	Photomicrograph of laminated calcite growth in discharge tubules of the tufa mound southwest of Moapa (sample MO-1) .	35
17.	XRD patterns compared for a discharge tufa mound southwest of Moapa (MO-1), for a sample 0.5 m deep in the outflow deposit from the tufa mound (MO-2) and for the surface of the outflow deposit immediately above sample MO-2 (MO-3). The progression from spring tufa to weathered deposit results in increased smectite (S) content. Quartz (Q) is detrital and forms one of the common nuclei for calcite ooids	36
18.	Photomicrograph of clear, botryoidal opal (opal-CT?) concentrated in the tops of voids between ooids and below a pebble in soil sample YW-2	39

19. Photograph of slope-parallel calcite-silica deposit in a sand ramp on the western flank of Busted Butte. Arrows mark a thin fault filling of calcite and silica that crosses the slope-parallel deposit. Depth from the ridge crest to the bottom of the ravine is 7.5 m. 41

20. XRD patterns comparing slope-parallel calcite-silica deposits at Fran Ridge (FR-6) and at Busted Butte (BB-1 and BB-3), a fault-filling calcite-silica deposit in the sand ramp at Busted Butte (BB-2), and standard room-temperature and glycolated smectite samples (BB-5 RT and glyc.) from the sand overlying sample BB-3. Minerals indicated are calcite (C), opal-CT (O-CT), clays (CL), smectite (S), and detrital quartz (Q) and feldspar (F) 42

21. Photomicrograph of fossil plant materials in sample BB-3. The cell walls are replaced by calcite and opal-CT; the cell interiors are filled by opal-CT 45

22. Photomicrograph of a fossil plant root (Larrea?) from the sand ramp along Fran Ridge near Trench 16. The cast formed by the living root is made of opal-A; infilling of the cast after plant death is of opal-CT 47

23. Comparative XRD patterns for slope-parallel sand ramp deposits (FR-6 and BB-3) and deposits from trenched faults (T-14 brown and TR-17) along the eastern flank of Yucca Mountain. The subequal abundances of calcite and opal-CT are characteristic of both depositional environments 49

A PRELIMINARY COMPARISON OF MINERAL DEPOSITS IN FAULTS NEAR
YUCCA MOUNTAIN, NEVADA, WITH POSSIBLE ANALOGS

by

D. T. Vaniman, D. L. Bish, and S. Chipera

ABSTRACT

Several faults near Yucca Mountain, Nevada, contain abundant calcite and opal-CT, with lesser amounts of opal-A and sepiolite or smectite. These secondary minerals are being studied to determine the directions, amounts, and timing of transport involved in their formation. Such information is important for evaluating the future performance of a potential high-level nuclear waste repository beneath Yucca Mountain. This report is a preliminary assessment of how those minerals were formed. Possible analog deposits from known hydrothermal veins, warm springs, cold springs or seeps, soils, and aeolian sands were studied by petrographic and x-ray diffraction methods for comparison with the minerals deposited in the faults; there are major mineralogic differences in all of these environments except in the aeolian sands and in some cold seeps. Preliminary conclusions are that the deposits in the faults and in the sand ramps are closely related, and that the process of deposition did not require upward transport from depth.

I. INTRODUCTION

Yucca Mountain, near the southwestern boundary of the Nevada Test Site in Nevada (Figs. 1A, B, and C), is being studied to determine its suitability to host a mined geologic repository for high-level radioactive waste. Research at Yucca Mountain, sponsored by the US Department of Energy and managed by its Waste Management Project Office at the Nevada Office of Operations, must address the question of seismic stability through the study of past fault movements near Yucca Mountain. Trenches have been excavated across faults near Yucca Mountain in order to assess the extent of Quaternary fault movement. In addition to fault displacements, these trenches revealed calcite and silica deposited in several of the faults. Figure 2 shows an example of one of the

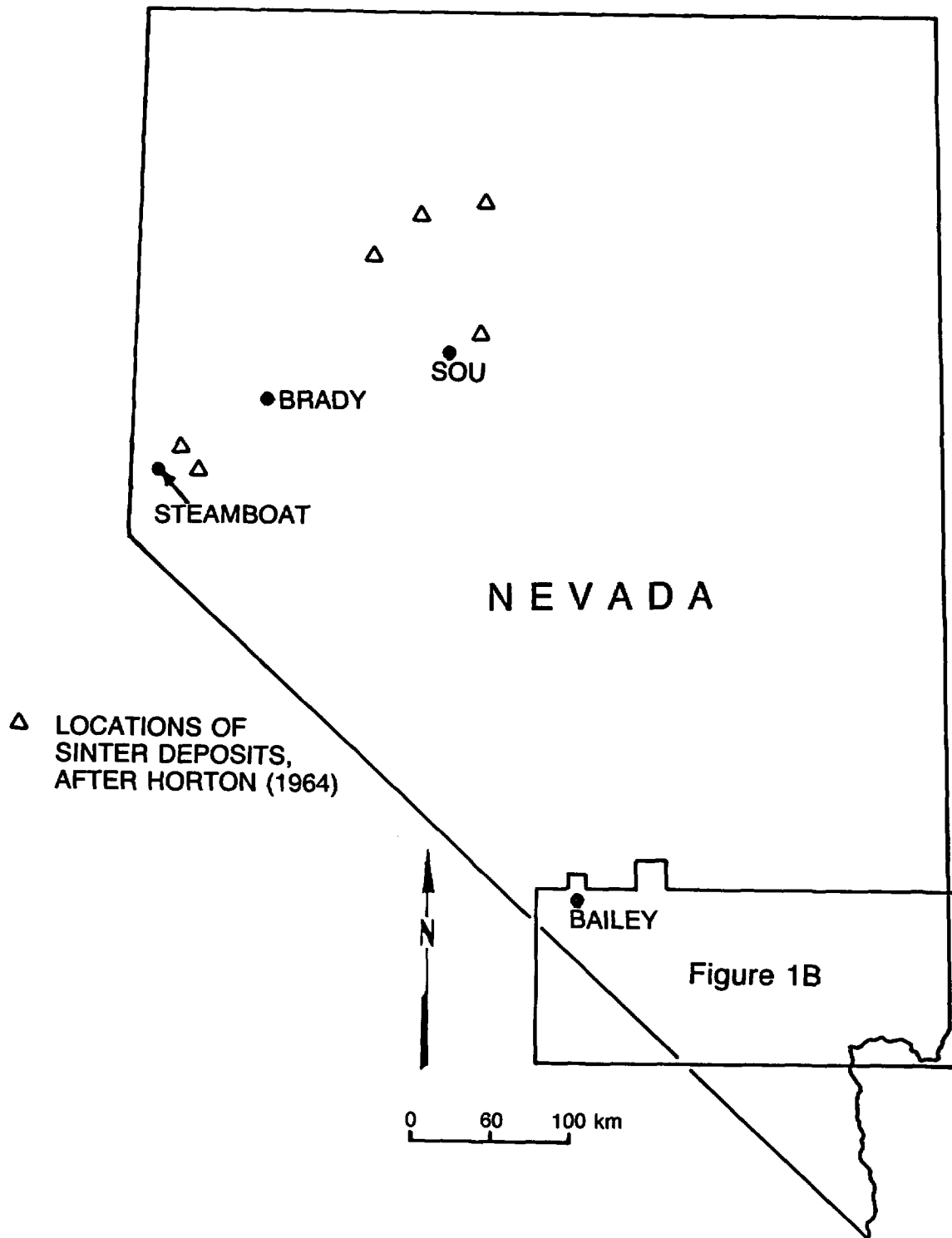


Fig. 1A.
 Locations of some warm springs (dots) and of warm-spring sinter deposits (triangles) in northern Nevada. The inset rectangle shows the area detailed in Fig. 1B.

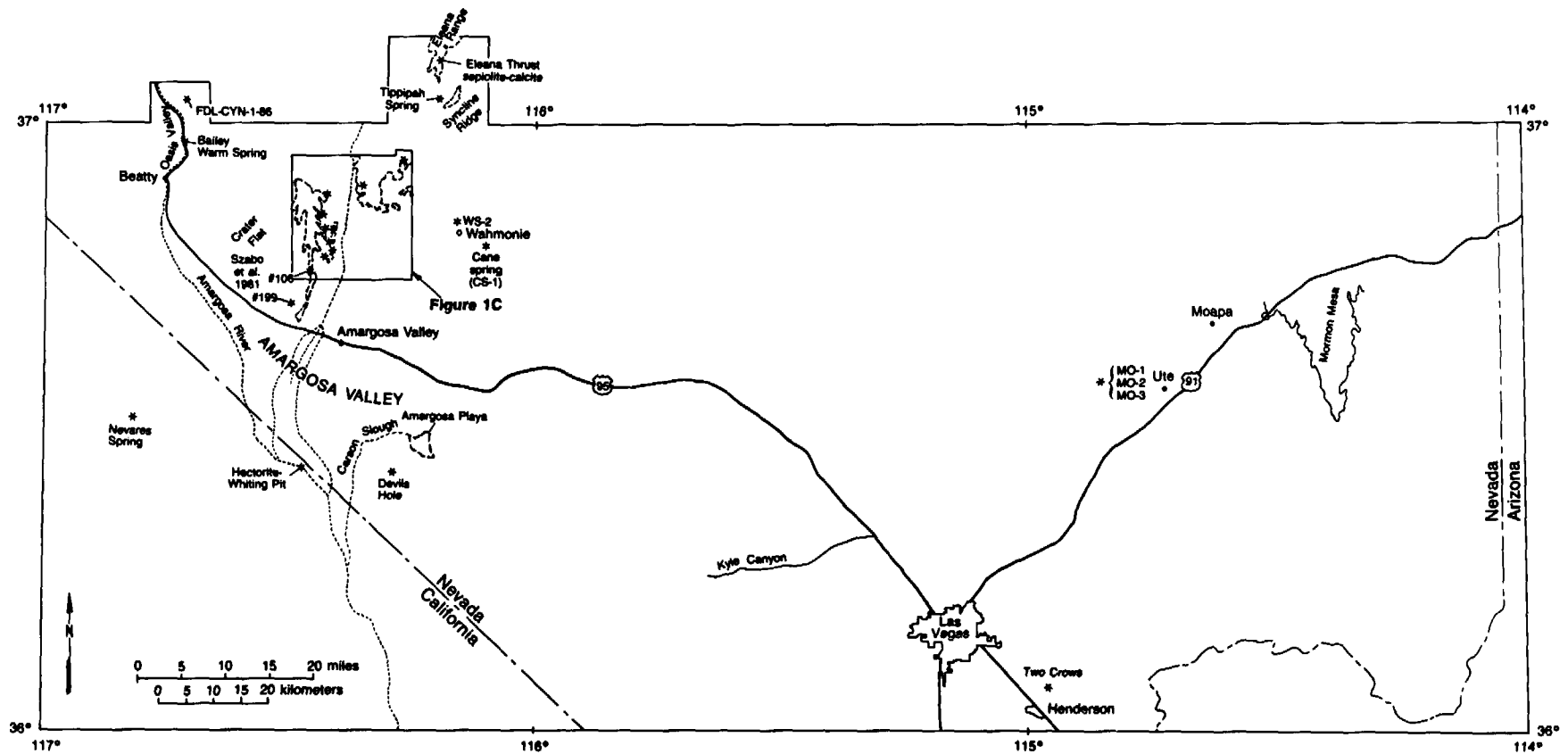


Fig. 1B.
 Sample localities mentioned in the text, other than those in northern Nevada
 (Fig. 1A) and near Yucca Mountain (Fig. 1C).

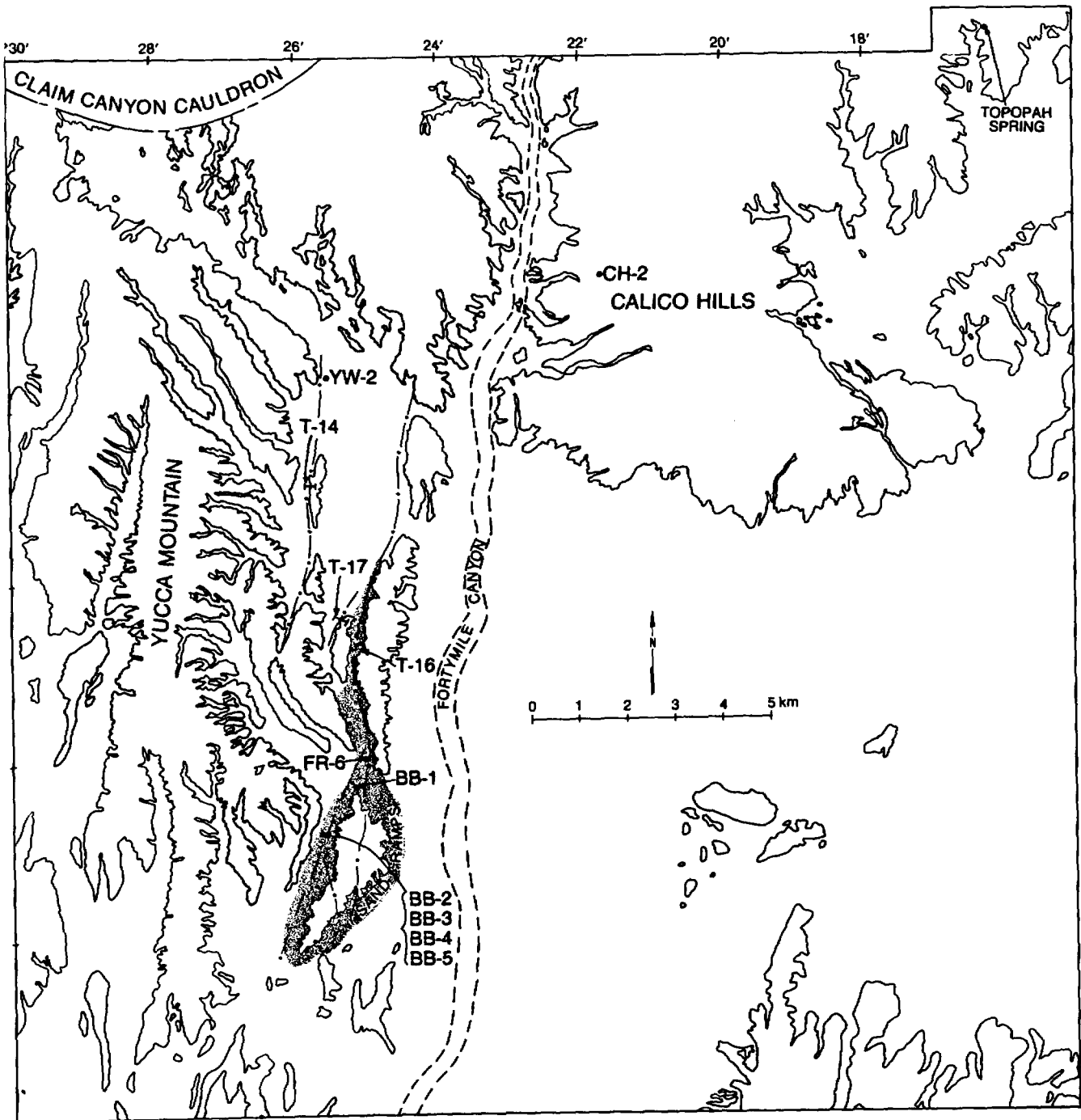


Fig. 1C.
Sample localities near Yucca Mountain.

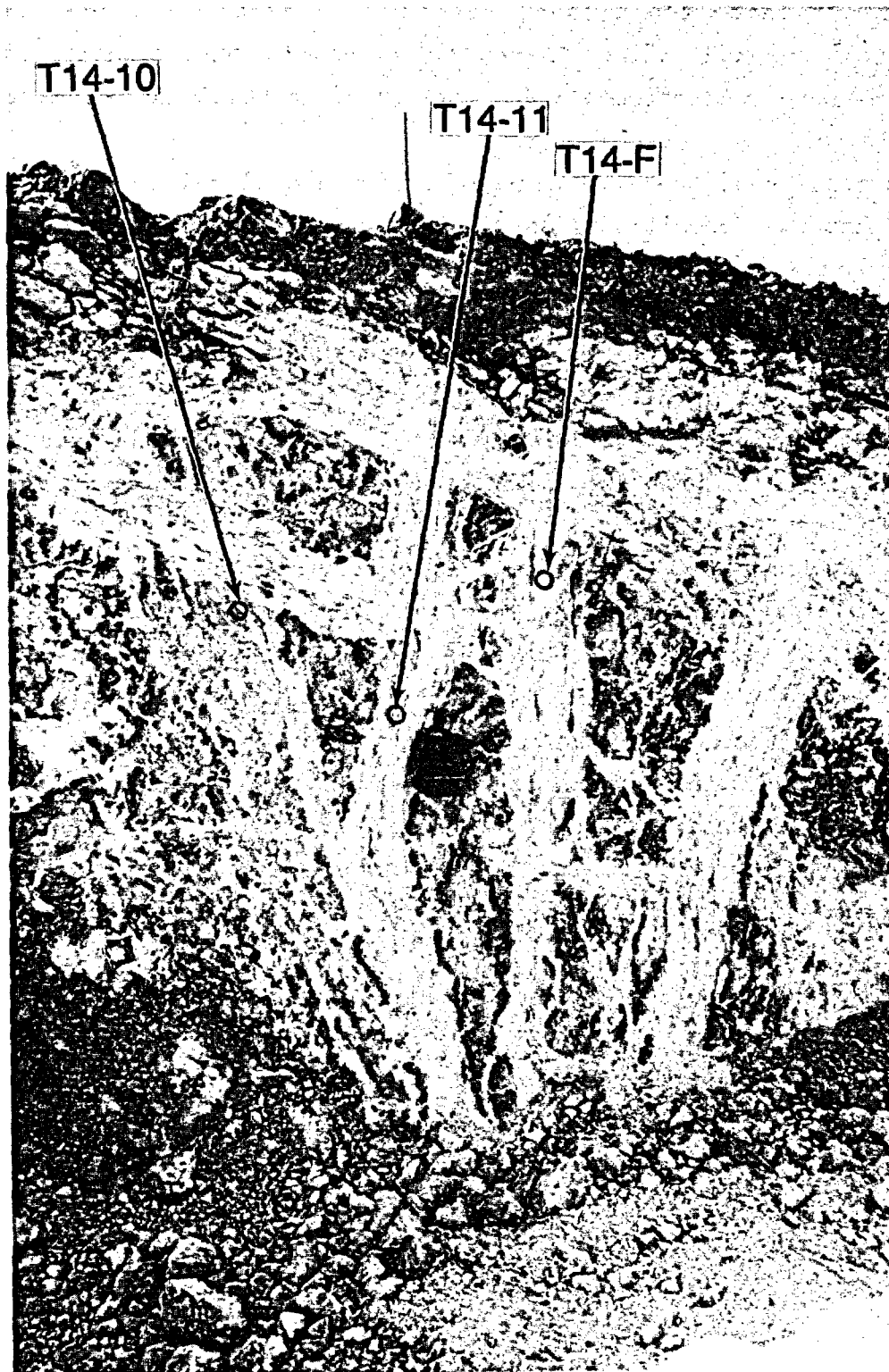


Fig. 2.
Photograph of the southern wall of Trench 14 with sample localities mentioned in the text. The notebook placed on the wall of the trench is 21 cm (8.5 in.) long.

widest of these deposits, exposed in the south wall of Trench 14 (Fig. 1C). The extent of those deposits of secondary minerals and the associated alteration of the tuff wall rocks were not expected. Subsequently, the origin of the deposits was questioned and a variety of depositional environments has been suggested.

Some studies of the secondary calcite and opal within trenched faults conclude that the depositional environment was limited to near-surface soil-zone transport and that the calcite and opal are mostly neofomed (Swadley and Hoover 1983; Taylor and Huckins 1986). However, Szabo et al. (1981) refer to similar materials as seep or spring deposits; these deposits have not been fully characterized (localities 106 and 199 in Fig. 1B). Workshops held on the fault-filling deposits have led to informal suggestions that the secondary minerals in the faults might be attributed to deep-seated hydrothermal or warm-spring activity. These suggestions of conflicting origin are difficult to evaluate because of an absence of full geological characterization of the secondary calcite-silica at Yucca Mountain. Furthermore, some mineralogic data are lacking for secondary minerals of known origin that might be used for comparison with the fault fillings at Yucca Mountain. In this paper we provide a preliminary mineralogic comparison between the fault-filling minerals at Yucca Mountain and possible analogs of known origin.

Five types of possible analogs for the Yucca Mountain fault fillings are described in this paper. The selection of analog types was based on consideration of a wide variety of fault- and fracture-related secondary calcite and silica in the area around Yucca Mountain. The five analog types are (1) near-surface exposures of hydrothermal vein deposits, (2) warm-spring or hot-spring deposits, (3) cold-spring or seep deposits, (4) soil deposits, and (5) aeolian "sand ramp" deposits. In terms of possible impact on an unsaturated repository beneath Yucca Mountain, the first two possible analogs have the strongest negative impact because they imply that deep, hot waters have risen upwards past the potential repository horizon. If the fault fillings are young, then such origins would be a serious concern. The third possible analog is of lesser concern, particularly if the possible spring or seep sources were perched rather than deep seated. Nevertheless, a spring or seep discharge from presently dry faults would require a re-evaluation of the presently assumed recharge rate of less than 0.5 to 4.5 mm/yr for Yucca Mountain (Montazer and Wilson 1984). The last two possible analogs impute a soil-development origin that requires no major deviations from the presently

observed arid processes at Yucca Mountain, with the possible exception of intermittent saturations during heavy rainfall accumulations. These soil-like origins would have no serious impact on an underlying repository. On the other hand, if the fault fillings have a seep or soil origin, then they might be useful to help calibrate the extent of near-surface transport along hydraulically conductive faults.

II. ANALYTICAL METHODS

Petrographic studies were made using polished thin sections in both transmitted and reflected light, at magnifications up to 500x. Electron microprobe analyses of calcite were made using a Cameca model CAMEBAX microprobe operated at 15-kV accelerating potential with a sample current of 5 nA. A ZAF data reduction routine was used, which assumed a fixed proportion of CO_2 in stoichiometric MCO_3 ($\text{MO} \cdot \text{CO}_2$).

X-ray diffraction (XRD) studies were made on rock powders using the bulk-sample methods of Bish (1981) and the clay mineral separation techniques described in Bish (in preparation). For analysis of calcite-rich samples, the calcite in a few samples was removed by dissolution in a bath of cold 10% HCl. Other analyses used the buffered pH 5 sodium acetate - glacial acetic acid dissolution as described by Jackson (1969). Clay minerals were separated by centrifugation or sedimentation. Because a variety of preparation methods was used on the samples described in this report, ranging from no treatment to acid dissolution and clay mineral separation, the preparation history of each sample is summarized in Table I.

III. RESULTS

The XRD data are summarized in Table II. Several of the minerals listed in Table II are not evident in the bulk samples analyzed but were found after the calcite fraction was removed, when the $<2\text{-}\mu\text{m}$ fraction was extracted, or when both treatments had been used. It is important to note that the minerals marked with circles in Table II are detrital or relic fragments that were not co-precipitated with the host deposit; the detrital or relic nature of these minerals was determined by petrographic analysis.

TABLE I

PREPARATION PROCEDURES USED FOR SAMPLES DESCRIBED IN THE TEXT

- Brady Springs tufa (RMV-201-82): crushed only.
- Busted Butte north side surface (BB-1): crushed only.
- Busted Butte west side surface (BB-3): crushed only.
- Busted Butte west side fault filling (BB-2): crushed only.
- Busted Butte west side fault filling (BB-2 2-5 μm acid): crushed, washed twice in pH 5 acetate buffer with Na-acetate rinses, rinsed in ethyl alcohol, treated in ultrasonic bath, sampled from precipitate after overnight settling.
- Busted Butte west side surface (BB-3 2-5 μm acid): crushed, washed twice in pH 5 acetate buffer with Na-acetate rinses, washed in ethyl alcohol, treated in ultrasonic bath, sampled from precipitate after overnight settling.
- Busted Butte west side surface (BB-3 1 day): sediment from supernatant over sample "BB-3 2-5 μm acid" after 24 hours settling time.
- Busted Butte west side buried sand (BB-4 $< 2 \mu\text{m}$): crushed, treated in ultrasonic bath, set aside overnight to allow settling of $> 2\text{-}\mu\text{m}$ fraction, collected from supernatant following evaporation.
- Busted Butte west side surface sand (BB-5 $< 2 \mu\text{m}$): crushed, treated in ultrasonic bath, set aside overnight to allow settling of $> 2\text{-}\mu\text{m}$ fraction, collected from supernatant after evaporation.
- Busted Butte west side surface sand (BB-5 oriented/glycolated): XRD of sample BB-5 $< 2 \mu\text{m}$ following preparation of oriented mount with ethylene glycol saturation.
- Calico Hills (CH-2): crushed only.
- Cane Spring (CS-1 white): crushed only.
- Fleur de Lis Canyon (FDL-CYN-1-86): crushed only.
- Fran Ridge (FR6): crushed only.
- Moapa spring mound (MO-1): crushed only.
- Moapa spring mound (MO-1 acidified): crushed, washed four times in pH 5 acetate buffer with Na-acetate rinses, rinsed in ethyl alcohol, sampled from precipitate after centrifuging 30 minutes at 9000 rpm.
- Moapa spring mound (MO-1 $< 2 \mu\text{m}$ acid): sampled from residue left after evaporation of supernatant from sample "MO-1 acidified."
- Moapa outflow at 3-ft depth (MO-2): crushed only.
- Moapa outflow at 3-ft depth (MO-2 acidified): crushed, washed four times in pH 5 acetate buffer with Na-acetate rinses, washed in ethyl alcohol, sampled from precipitate after centrifuging 30 minutes at 9000 rpm.
- Moapa outflow at 3-ft depth (MO-2 $< 2 \mu\text{m}$ acid): sampled from residue left after evaporation of supernatant from sample "MO-2 acidified."
- Moapa outflow surface (MO-3): crushed only.
- Moapa outflow surface (MO-3 acidified): crushed, washed four times in pH 5 acetate buffer with Na-acetate rinses, washed in ethyl alcohol, sampled from precipitate after centrifuging 30 minutes at 9000 rpm.
- Moapa outflow surface (MO-3 $< 2 \mu\text{m}$ acid): sampled from residue left after evaporation of supernatant over sample MO-3 acidified.
- Moapa outflow surface (MO-3 $< 2 \mu\text{m}$ oriented): XRD of oriented mount made from sample MO-3 $< 2 \mu\text{m}$ acid.
- Moapa outflow surface (MO-3 $< 2 \mu\text{m}$ oriented/glycolated): XRD of glycolated mount MO-3 $< 2 \mu\text{m}$ oriented.

TABLE I (cont)

Nevares Spring (Nevares): crushed only.
 Steamboat Springs altered rock (RMV-205-A): crushed only.
 Steamboat Springs sinter (RMV-205-D): crushed only.
 Trench 14 silica band in fault (T14-FA silica): crushed only.
 Trench 14 fault (T14-FA,R): crushed only.
 Trench 14 fault (T14-FA,R acidified): crushed, washed twice in pH 5 acetate buffer, rinsed in sodium acetate, rinsed in deionized water, sampled from residue.
 Trench 14 fault (T14-FB calcite): crushed only.
 Trench 14 fault (T14-FB insoluble): crushed, insoluble residue sampled after treatment in cold 10% HCl and NaOH neutralization.
 Trench 14 fault (T14-FB >2 μm insoluble): neutralized supernatant collected over sample T14-FB insoluble, sample collected after sedimentation overnight.
 Trench 14 fault (T14-FB >2 μm glycolated): XRD of oriented and glycolated mount prepared from sample "T14-FB >2 μm insoluble."
 Trench 14 fault (T14-FB <2 μm insoluble): crushed, dissolved in cold 10% HCl, neutralized in NaOH, ultrasonic bath followed by separation of <2- μm fraction through gravitational settling.
 Trench 14 fault (T14-FB <2 μm glycolated): XRD of oriented and glycolated mount prepared from sample T14-FB <2 μm insoluble.
 Trench 14 fault center (T14-11 white): crushed only.
 Trench 14 fault center (T14-11 brown): crushed only.
 Trench 14 wall (T14-10 gdms): crushed only.
 Trench 14 wall (T14-10 gdms <2 μm acid): crushed, washed twice in pH 5 acetate buffer with sodium acetate rinses, rinsed in ethyl alcohol, centrifuged at 9000 rpm for 20 minutes, sample taken from supernatant after evaporation.
 Trench 14 wall (T14-10 acidified): precipitate from final centrifugation of sample "T14-10 gdms <2 μm acid."
 Trench 14 wall contact (T14-10 vein): crushed only.
 Trench 14 wall contact (T14-vein acidified): crushed, washed in cold 10% HCl, neutralized in NaOH, sampled from precipitate.
 Trench 16 root (T16-1 rim): crushed only.
 Trench 16 root: (T16-1 core): crushed only.
 Trench 17 fault (T17-1): crushed only.
 Trench 17 fault (T17-1 acid residue): crushed, insoluble residue sampled after treatment in cold 10% HCL and NaOH neutralization.
 Wahmonie deposit (WS-2 bulk): crushed only.
 Wahmonie deposit (WS-2 acid flocculant): crushed, washed in cold 10% HCl for 30 minutes, neutralized in NaOH, sample taken from residue left after evaporation of supernatant.
 Yucca Wash (YW-2): crushed only.
 Yucca Wash (YW-2 acidified): crushed, washed four times in pH 5 acetate buffer with Na-acetate rinses, rinsed in ethyl alcohol, sampled from precipitate after centrifuging for 30 minutes at 9000 rpm.
 Yucca Wash (YW-2 <2 μm acid): sampled from residue after evaporation of supernatant from sample "YW-2 acidified."
 Yucca Wash (YW-2,R): crushed only.
 Yucca Wash (YW-2,R acidified): crushed, washed twice in pH 5 acetate buffer, rinsed in sodium acetate, rinsed in deionized water, sampled from residue.

TABLE II
X-RAY DIFFRACTION DATA^a

	Calcite	Opal-A	Opal-CT	Opal-C	Quartz	Clay	Cryptomelane	Gypsum	Halite	Burkeite	Trona	Feldspar	Mica
Yucca Mountain Faults													
T14-FA	X	X	X										
T14-FA,R	X	X											
T14-FB	X		X		0	S							
T14-10 gds	X		X		0	X						0	
T14-10 vein	X		X		0								
T14-11	X		X										
TR17	X		X		0	X							
Hydrothermal Vein													
CH-2				X	X		X						
Warm-Spring Deposits													
RMV-201-82		X											
FDL-CYN-1-86									X	X	X		
RMV-205-D		X											
WS-2	X					X		X				0	
Cold Springs and Seeps													
CS-1	X				0							0	
MO-1	X												
MO-2	X				0	X							
MO-3	X				0	X							
Nebares	X												0
Soil													
YW-2 and 2,R	X	X	X		0	X						0	0
Sand Ramps													
BB-1	X		X		0	X						0	
BB-2	X		X		0	X						0	
BB-3	X		X		0	X						0	
BB-4 ^b						X							
BB-5 ^b						X							
FR6	X		X		0	X							
T16-1 Rim		X											
T16-1 Core			X										

^a X = authigenic; 0 = relic or detrital based on optical examination; S = positive sepiolite identification.

^b Only the <2- μ m fraction was x-rayed in BB-4 and BB-5.

Several comparative petrographic features are listed in Table III. The term "ooids" is used throughout this paper to describe any pelletal or spherical forms smaller than 2 mm; these features may be massive but are typically formed of distinct concentric growth layers, and they may or may not have foreign nuclei of rock, mineral, or glass fragments. Where opal is visible, a distinction is made between a single opal type or multiple types, based on variations in color, relief, birefringence, or growth forms. Any remains of fossil vascular plants either in thin section or in outcrop are noted. The term "geopetal opal" is used to describe distinct opal concentrations on the undersides of pebbles. Deposits that are layered on a millimeter scale are said to have laminae, and cross-cutting laminae representing disruption between depositional series are noted. Occurrence of quartz formed in situ rather than by accidental inclusion is also noted. The preservation of accidental pumice fragments is recorded. Finally, the occurrence of discharge flow-tube structures in spring mounds is recorded. Each sample studied is variable and often complex beyond the simple categorization of Table III; therefore this table is only a summary of some of the most prominent features. Electron microprobe data for calcite were obtained only where crystals coarser than micrite were found (Table IV). Many of the petrographic details are discussed along with the corresponding XRD data for each sample in the section that follows, and electron microprobe data are discussed where appropriate.

IV. DISCUSSION

Our discussion of the XRD and petrographic data is organized to follow the six types of localities listed along the left sides of Tables II and III. First, the samples analyzed from the faults around Yucca Mountain are discussed. Then the samples from the five possible analogs (hydrothermal veins, warm-spring deposits, cold-spring and seep deposits, soils, and sand ramps) are discussed. As part of the discussion, published studies and personal communications are cited where they are relevant to the minerals in faults and to the possible analogs. Much work has already been done in southern Nevada on many of these mineral associations, and these previous studies are important to the interpretations and conclusions made in this paper.

TABLE III
PETROGRAPHIC DATA

	Ooids	Single Opal Type	Multiple Opal Types	Fossil Vascular Plants	Geopetal Opal	Laminae	Cross-Cutting Laminae	Co-Deposit of Euhedral Quartz	Pumice Fragments	Flow Tube Structure
Yucca Mountain Faults										
T14-FA	X		X	X			X			
T-14-FA,R	X	X		X						
T14-FB	X		X			X				
T14-8 ^a	X	X							X	
T14-10	X		X			X				
T14-11	X		X			poor				
T17-1	?		X				X			
Hydrothermal Vein										
CH-2		X						X		
Warm Springs										
RMV-205-D		X				X				
San Ignacio		X		X						
Cold Springs/Seeps										
MO-1	X			X		X				X
MO-2	X					X				
MO-3	X					X				
Nebares				X						
Soil										
YW-2 and 2,R	X		X		X	X				
Sand Ramps										
BB-2	?		X			X			?	
BB-3	?		X	X		poor			X	
FR-6	X		X	X		X			?	
T16-1 ^b			X	X					X	

^a T14-8 is a sample of loose volcanic ash and detrital fragments, with incipient ooidal rinds of calcite and opal-CT.

^b T16-1 is a root cast and opal infilling (cf. Fig. 22).

TABLE IV
ELECTRON MICROPROBE ANALYSES OF CALCITES

wt% oxide	<u>Nevarés</u>	<u>Moapa M0-1</u>	<u>Moapa M0-2</u>	<u>Trench 14 wall (T14-10 gdms)</u>
CaO	53.5	54.8	54.5	55.9
MgO	2.20	0.82	1.20	0.55
FeO	0.06	0.00	0.00	0.04
MnO	0.00	0.03	0.00	0.02
SrO	0.21	0.01	0.00	0.08
BaO	0.00	0.13	0.03	0.00
CO ₂ ^a	44.1	44.2	44.3	43.4
Total	100.1	100.0	100.0	100.0
cations/3 oxygens				
Ca	0.949	0.975	0.967	1.002
Mg	0.054	0.020	0.030	0.013
Fe	0.001	0.000	0.000	0.000
Mn	0.000	0.000	0.000	0.000
Sr	0.002	0.000	0.000	0.001
Ba	0.000	0.001	0.000	0.000
C ^a	0.997	1.002	1.001	0.991
Total	2.003	1.998	1.998	2.007

^aCO₂ calculated by difference from 100 wt%.

A. Deposits Within Faults Near Yucca Mountain

Several faults have been exposed by trenching and mapped around Yucca Mountain (Swadley and Hoover 1983; Szabo and O'Malley 1985), and several of these faults contain deposits of calcite, silica, and clay minerals. These deposits consist of many small depositional bands, some of which are cross cutting. The banded nature indicates that the minerals were probably deposited by a process that was repetitive and persisted over a long time span. Alteration of the tuff wall rock to calcite, silica, and clay minerals is also found; this alteration is evaluated in the discussion of sample T14-10. The descriptions below concentrate on two of the faults in which these mineral deposits and the alteration effects in the wall rock are most extensive. The faults studied are those exposed in Trenches 14 and 17 (Fig. 1C).

1. Samples from Trench 14. The largest of the deposits studied is exposed in Trench 14 (Fig. 2). Samples T14-F and T14-11 were collected within the banded central regions of two of the fault splays exposed in the southern wall of Trench 14. Sample T14-10 was collected a few feet east of the other samples and includes the contact between minerals deposited along the fault and the altered wall rock. The wall rock at this point is the densely welded and devitrified Tiva Canyon Member of the Paintbrush Tuff.

Sample T14-F

Interpretations of the banded sample T14-F indicate that there were at least two episodes of deposition, as illustrated in Fig. 3. The earlier episode (T14-FB) is represented by very complex layering of patchy, mineral-clast rich, fragmental, and ooidal layers. These layers are, individually, 1 mm to 1 cm thick; the thicker layers are themselves formed of layered clasts up to a few millimeters long, indicating that even earlier deposition has occurred followed by brecciation and recementation. Ooids are 0.1 to 0.4 mm in diameter with few detrital nuclei (see Hay and Wiggins 1980 for a discussion of ooidal textures). The abundant mineral clasts that occur in some layers are widely varied but include fragments of quartz, potassium feldspar, plagioclase feldspar, amphibole, olivine, clinopyroxene, and both clear and colored volcanic glasses. The later episode of deposition (T14-FA) was much simpler and consists of almost pure laminated opal, which cuts across the earlier layering. The younger deposit appears to have begun with a minor amount of microcrystalline calcite (crystals smaller than 0.1 mm) but is dominated by almost pure opal layers. X-ray diffraction analysis (Fig. 4) shows that this opal is amorphous (opal-A in the nomenclature of Jones and Segnit 1971) and differs markedly from the calcite-rich ooidal layers of the earlier depositional episode.

The nature of opal structural types is an important parameter in describing the deposits in faults, hydrothermal veins, warm springs, soils, and sand ramps. Opal XRD data will be compared throughout this paper. Three opal structural types are commonly identified based on the work by Jones and Segnit (1971); these three types range from amorphous (opal-A) to opal with short-range tridymite and cristobalite-type stacking (opal-CT) to opal with more extensive domains of cristobalite-type stacking (opal-C). XRD patterns of these three opal structural types are illustrated in Fig. 5 for comparison with XRD patterns used in this paper.

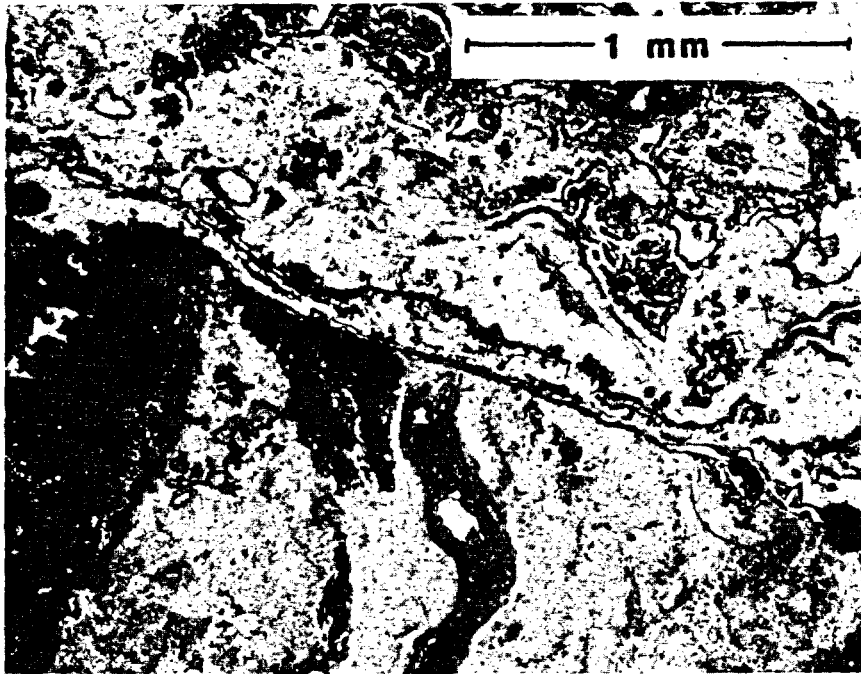


Fig. 3.

Photomicrograph of sample T14-F. The clear band of opal-A (sample split T14-FA) overlies earlier layers of calcite with opal-CT (sample split T14-FB).

The youngest depositional episode in sample T14-F consists of opal-A. Another split from this youngest layer (sample T14-FA,R) was analyzed to confirm the identification of opal-A. Aside from being somewhat more transparent than the other relatively pure opal zone in Trench 14, the opal-A in sample T14-F differs in having remnants of organic structures (note inset photomicrograph in Fig. 4). Remnants of small root cases can be seen in hand samples of the opal-A. The earlier episode of complex layered deposition in T14-F and in all other calcite-silica banding found in the faults is opal-CT. The opal-CT does not preserve any organic structures of hand-sample or thin-section scale.

Figure 6 is the XRD pattern of the $<2\text{-}\mu\text{m}$ -size fraction separated from the earlier-episode layers (T14-FB). This pattern shows the presence of the mineral sepiolite. Coarsely crystalline sepiolite can form in hydrothermal environments as fibrous crystals up to 5 cm long (Imai and Otsuka 1984). Post (1978) described a nearly pure vein filling of sepiolite at Two Crows, east of Henderson, Nevada, (Fig. 1B) and suggested an origin by direct precipitation from deep water sources; he did not rule out a hydrothermal origin for this

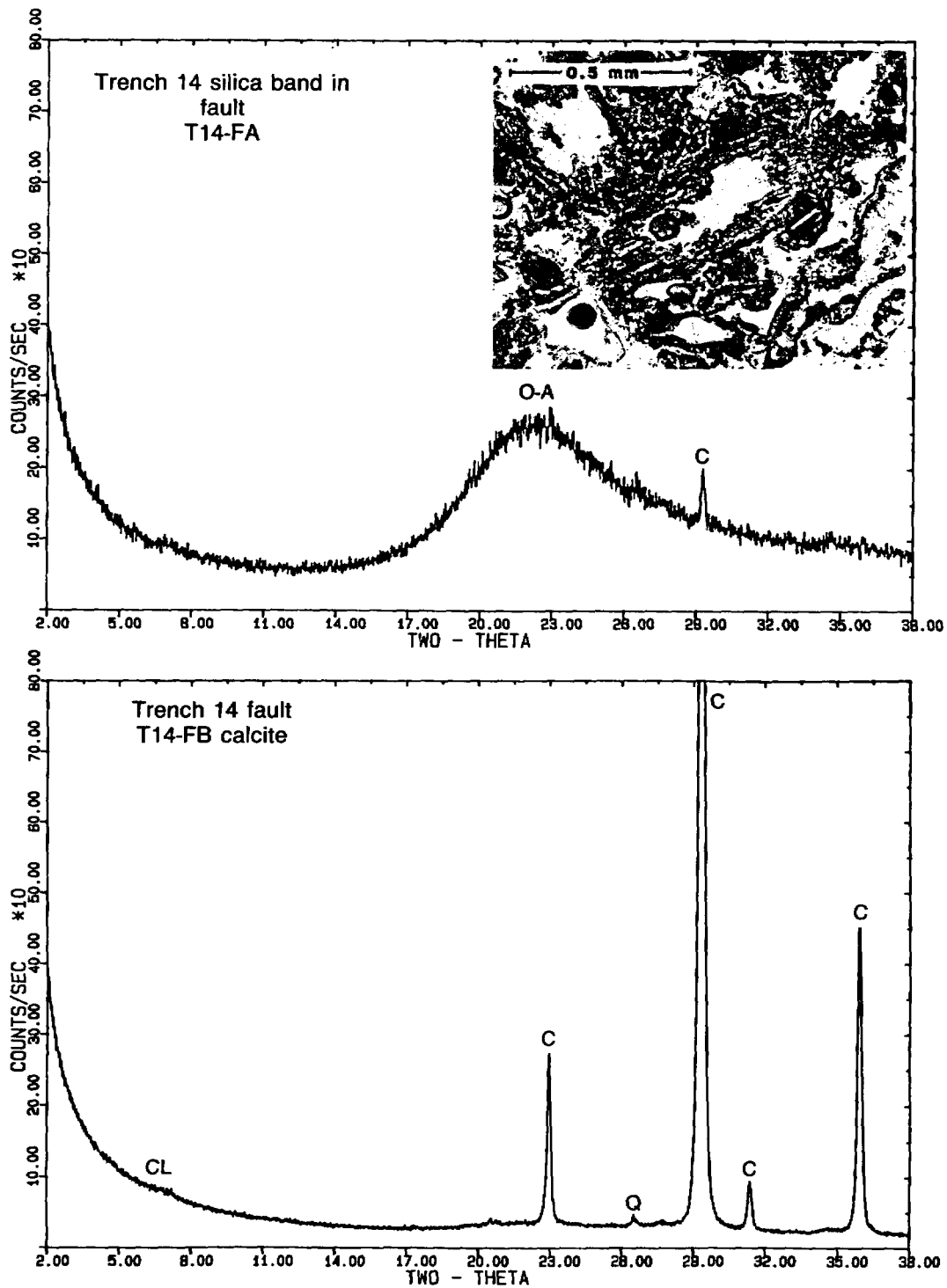


Fig. 4.

XRD patterns of T14-FA and T14-FB compared. The peaks labeled are calcite (C), opal-A (O-A), quartz (Q), and clay (CL). The inset photomicrograph shows remnant organic structure within the opal-A of T14-FA; all structures shown consist of opal.

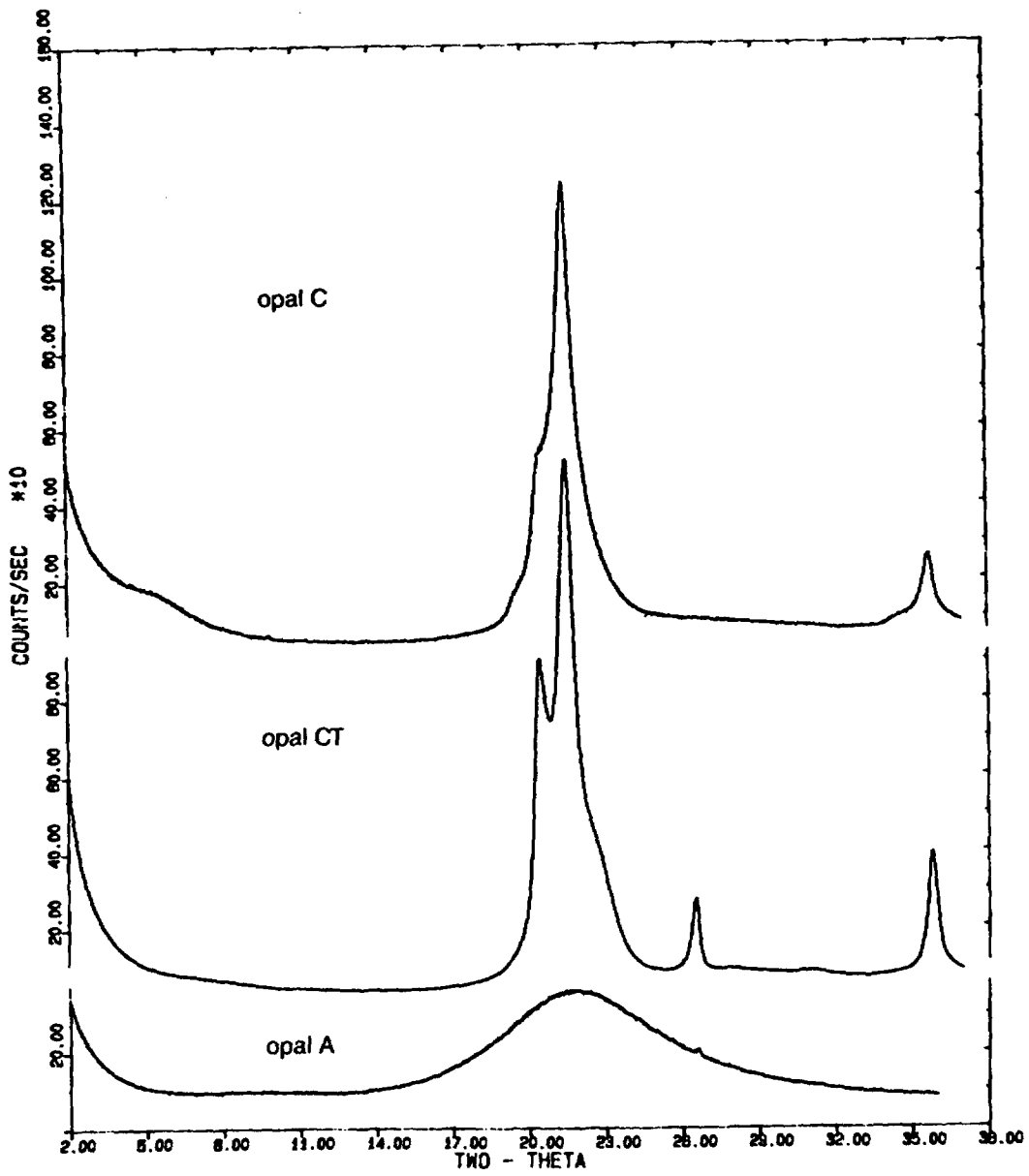


Fig. 5.
Comparative XRD patterns of opal-A, opal-CT, and opal-C.

deposit. However, Post also contrasted the pure sepiolite at Two Crows with a sepiolite-dolomite duripan in North Las Vegas and, closer to Yucca Mountain, a sepiolite-dolomite playa deposit in the Amargosa Valley (Fig. 1B). In these other localities Post suggested that the sepiolite precipitated directly from high-Mg, high-pH surface waters. Jones (1983) examined the distribution of sepiolite and smectite around Yucca Mountain and suggested that sepiolite can be formed by precipitation in playas, spring seeps, old soils, and faults (Fig. 7) but that it is also commonly redistributed by aeolian processes. Thus the occurrence of sepiolite is not definitive evidence of a particular origin, although the commonest occurrences of sepiolite in Southern Nevada appear to be either playa formed or pedogenic. With further study the data on sepiolite abundance, size, form, composition, and associated mineral assemblages may provide some constraints on origin.

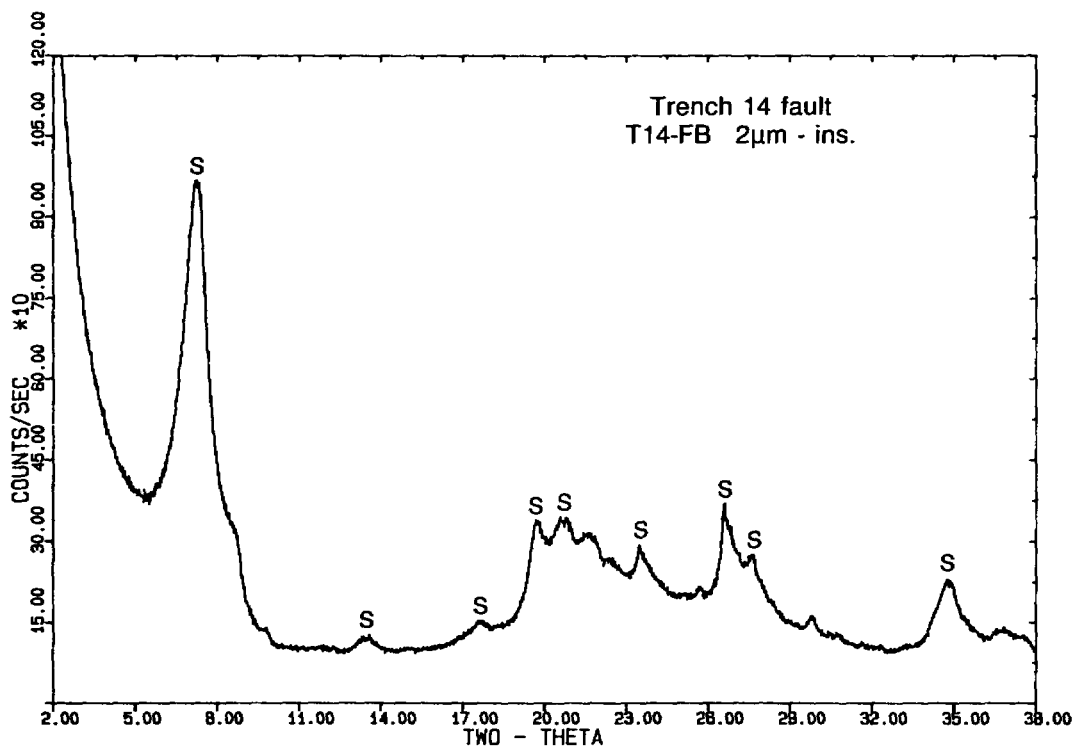


Fig. 6.

XRD pattern of sepiolite (S) in the <2- μ m-size fraction of sample T14-FB.

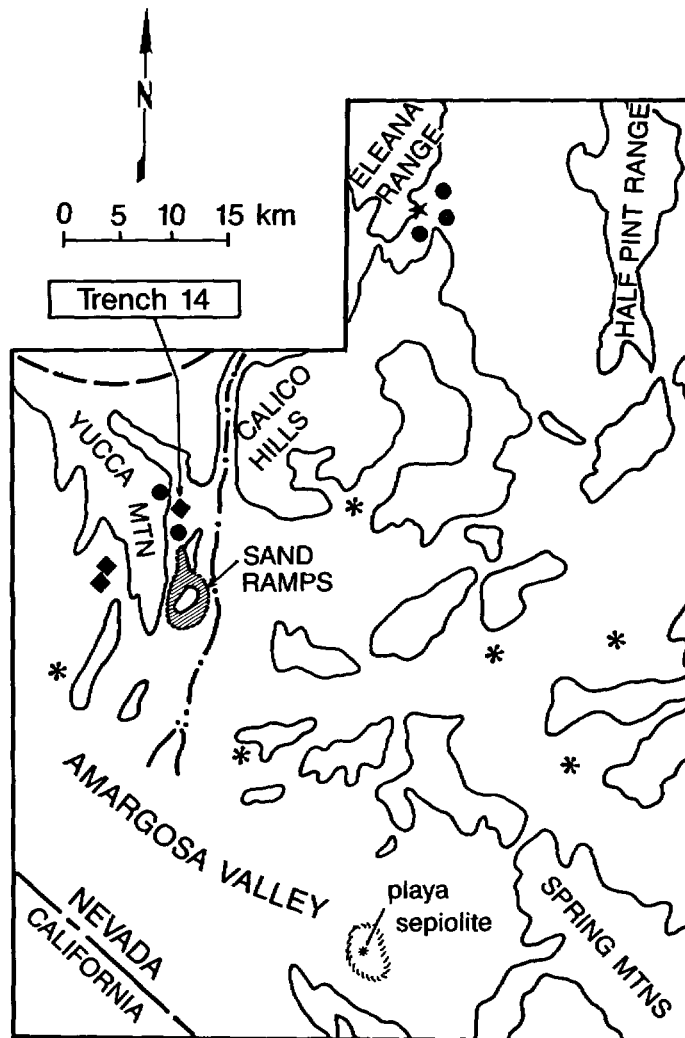


Fig. 7.
 A map of chain-structure clay (sepiolite) distributions in soils, faults, and a spring seep around Yucca Mountain (after Jones 1983). The locality of Trench 14 and of sand ramps south of the trench is also shown.

Sample T14-11

The more typical banded deposits within the fault at Trench 14 consist of parallel layers of dense buff-colored calcite and opal-CT with minor concordant layers of white or colorless, relatively pure opal-CT. Sample T14-11 (Fig. 2) contains such layering, and the layers are compared in Fig. 8. The central calcite-silica band is about 1 cm wide, and the outer layers of relatively pure opal are 0.5 to 3 mm thick.

The outer layers of pure opal-CT in sample T14-11 were deposited after the calcite-silica layer; this is the same relative timing of deposition as was seen in sample T14-F (above) in which pure silica deposition is a relatively recent event, although in T14-11 the pure silica is opal-CT rather than opal-A. We cannot rule out the possibility that the pure silica layers in T14-11 may have originally been formed as opal-A, possibly as organic structures as in samples T14-FA and T14-FA,R. The late deposition of relatively pure opal is seen throughout Trench 14, in other fault-related deposits in the sand ramps, and in the soils around Yucca Mountain. In contrast, pure opal deposition is an early and ongoing feature in sinter deposits from warm springs and does not appear to occur at all in cold-spring or seep deposits. However, small amounts of euhedral quartz occur in the Hectorite-Whiting spring deposits of the Amargosa Valley (Fig. 1B; Khoury et al. 1982), and larger amounts of opal-CT, chalcedony, and quartz occur as a result of groundwater-caused silicification and replacement of playa carbonates and clays near Carson Slough in the Amargosa Valley (Fig. 1B; Hay et al. 1986).

Sample T14-10

Sample T14-10 provides an important comparison between layered silica-rich deposits along the wall of the fault and relatively calcite-rich alteration of the tuff wall rock (Fig. 9). The altered tuff consists of small brecciated tuff fragments (less than 0.5 cm in diameter) from the devitrified Tiva Canyon member, with matrix replacement by the coarsest calcite crystals (10 μ m long) yet observed in Trench 14. The calcite crystals are also unique because of their euhedral habit (doubly terminated spar). The coarse size of these calcite crystals has permitted electron microprobe analysis, and the results are tabulated in Table IV along with calcite analyses from two spring deposits. All are low-Mg or closely similar intermediate-Mg calcites, with no major differences in composition detectable by electron microprobe analysis. The fabric of calcite growth in the altered tuff suggests invasion along fractures between breccia fragments, although some replacement growth is suggested by

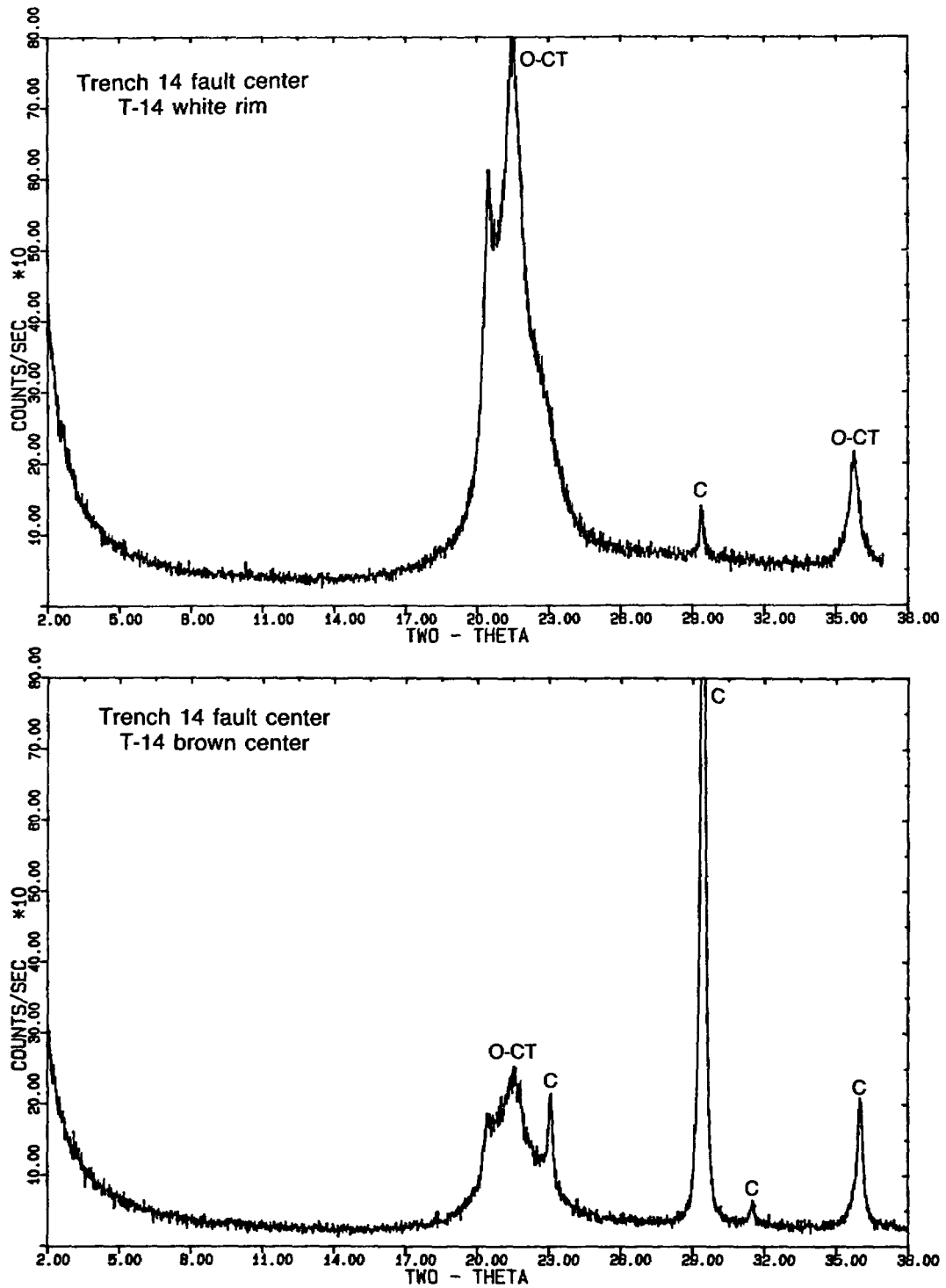


Fig. 8.
 XRD patterns comparing the calcite (C) and opal-CT (O-CT) of a dense calcite-silica band (T14-11 brown) and its outer coating of laminated botryoidal opal-CT (T14-11 white).

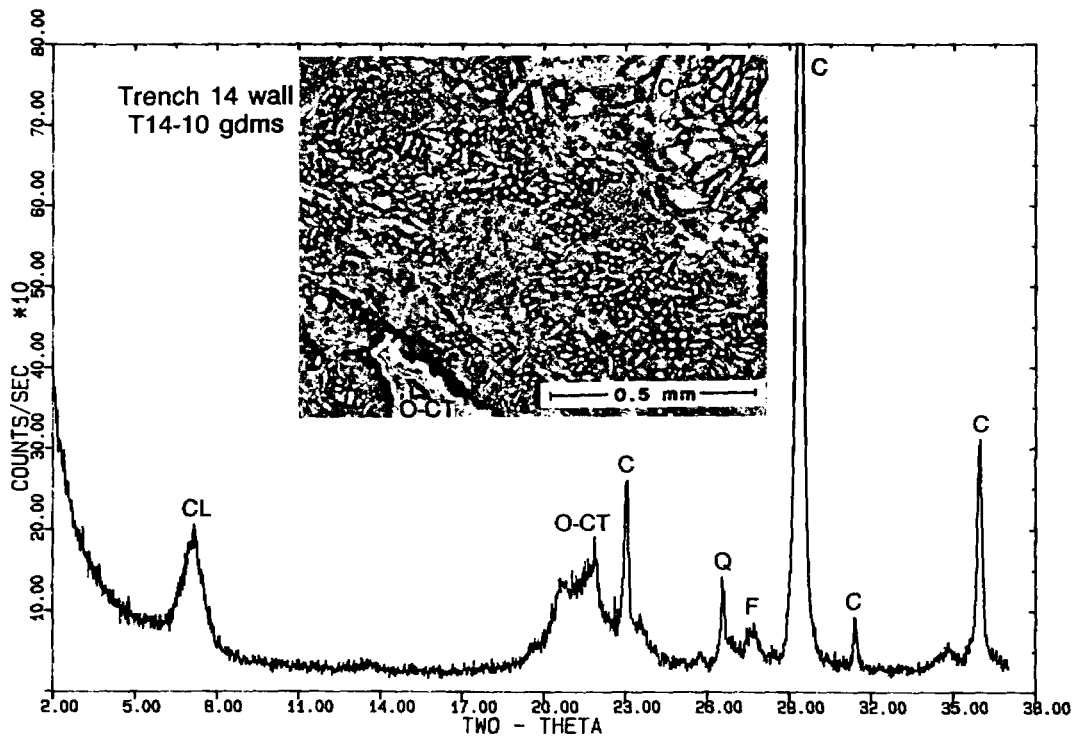
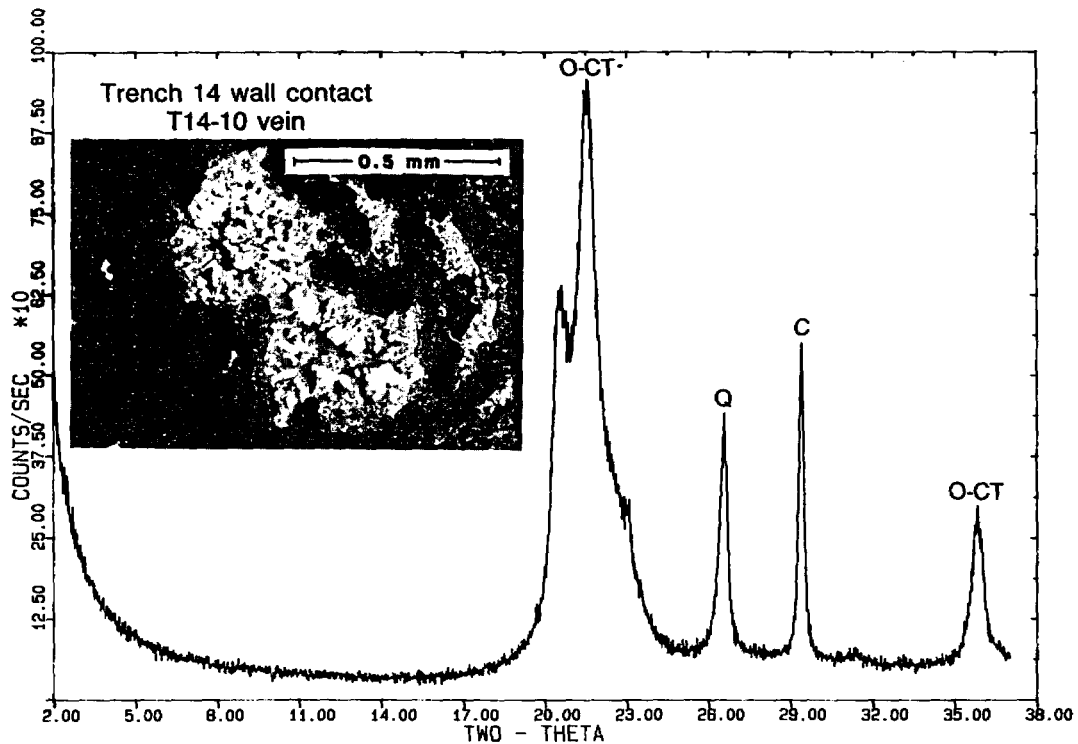


Fig. 9.

XRD patterns comparing the fault deposit (T14-10 vein) and the adjacent matrix of the altered tuff (T14-10 gdm) at a locality within the altered Tiva Canyon member in Trench 14 (Fig. 2). The minerals shown are calcite (C), opal-CT (O-CT), quartz (Q), and clay (CL). Inset photomicrographs show representative textures of the two samples. The photomicrograph of T14-10 vein shows both colloform and coarse birefringent opal. The photomicrograph of T14-10 gdm shows calcite crystals (C) and late opal (O-CT).

calcite embayments in tuff fragments and by remnant phenocrysts surrounded by calcite crystals. Opal-CT occurs along the walls of many of the voids between clusters of calcite crystals, although a final void filling of calcite in some cases suggests that calcite deposition occurred more than once. There are several opal morphologies, including colloform and massive birefringent forms. The variability in opal morphologies and optical properties suggests that the opal-CT seen in the XRD pattern is an averaged pattern representing several opal structural types. The broad diffraction maximum at $7.1^\circ 2\theta$ indicates relatively abundant clay, although study of the less than $2\text{-}\mu\text{m}$ fraction has not been able to resolve whether this is a chain-structure clay such as sepiolite or a smectite.

The layered silica deposited in contact along the wall of the altered tuff contains microcrystalline calcite-silica layers intercalated between relatively pure silica layers. The XRD pattern for this layered silica deposit shows a relatively sharp opal-CT diffraction band centered over $21.59^\circ 2\theta$. As in the adjacent altered tuff, this opal diffraction pattern represents an average of more than one opal type. The inset photomicrograph of the layered silica deposit (T14-10 vein in Fig. 9) shows at least two types of opal on a microscopic scale, with massive or colloform colorless opal of moderate birefringence deposited on earlier brown colloform opal. A sharp quartz diffraction peak is also seen in this XRD pattern, but this peak is due to broken fragments of earlier drusy quartz that have been incorporated into the layered silica deposit.

Drusy Quartz in Trench 14

Euhedral quartz crystals form encrustations (i.e., drusy quartz) on many of the cavities in the Tiva Canyon Member exposed in Trench 14. The age of these relatively coarse (up to 0.5 cm) quartz crystals is of interest because their relation (if any) to the later opal deposition within the fault will have a bearing on the interpretation of the calcite-silica deposits. Drusy quartz crystals have been collected from Trench 14 for fluid inclusion and stable isotope studies and to attempt age determination by electron spin resonance. Preliminary data suggest a relatively high temperature of formation (D. Vaniman, letter to D. Vieth, July 1985). The occurrence of a significant peroxy-defect electron spin resonance signal suggests that the drusy quartz is not young (S. Levy, personal communication, September 1986). The distribution of drusy quartz in Trench 14A, just north of Trench 14, is revealing; here two different tuffs, the Tiva Canyon Member (12.4-My age) of the Paintbrush Tuff

and the Rainier Mesa Member (10.4-My age) of the Timber Mountain Tuff, occur on opposite sides of the fault. As in Trench 14, the drusy quartz is found in place in the Tiva Canyon wall rock and as broken fragments dragged into the fault along with the tuff. In Trench 14A, however, there is the added constraint that the drusy quartz is not found in the Rainier Mesa wall rock. These relations indicate that the drusy quartz predates most if not all of the calcite-silica deposits of the fault (in which it occurs only as accidental fragments) and predates the juxtaposition of Tiva Canyon and Rainier Mesa tuffs along the fault (S. Levy, personal communication, August 1986). Actual dating and interpretation of the drusy quartz occurrence is of considerable interest because this material is widespread throughout the Tiva Canyon Member and near the base of the Topopah Spring Member at Yucca Mountain, but the evidence so far available indicates that it is a deposit considerably older than the calcite-silica and silica layering within the faults studied in trenches.

2. Sample from Trench 17. A sample from Trench 17 (Fig. 10) is described here for comparison to the Trench 14 samples to illustrate the lateral uniformity in mineral composition but variation in texture of the fault deposits along the flank of Yucca Mountain. Within the fault exposed in Trench 17 the total width of the calcite-silica deposit is less (about one meter), and small-scale banding of calcite-silica and silica depositional layers does not occur as in Trench 14. Instead, the fault-filling deposit is a single complex brecciated mass of opal-CT and calcite, with fragments of tuff and of drusy quartz crystals as described in Trench 14. Ooidal structures are almost completely absent, although many of the calcite-silica clasts incorporated in the deposit have an enigmatic structure of small (0.05 - 0.1 mm) aligned polygonal cells, which are often curving or concentric (relic ooids?; see inset photomicrograph in Fig. 10). Despite the strikingly different texture, the mineralogy of the sample from Trench 17 is virtually identical to the predominant mineralogy (calcite, opal-CT, and minor clay) of Trench 14 (compare the upper part of Fig. 10 with the upper part of Fig. 9). Opal-A, however, has not been found in the fault deposit of Trench 17. Neither have organic structures been found in either hand sample or thin section. The similarity in major mineralogy with Trench 14 indicates that although the calcite-silica deposits in the faults are texturally very complex and include a wide variety of brecciated and detrital rock and mineral fragments, the deposits that actually crystallized from solution within the faults are consistently composed of calcite and opal-CT with minor amounts of sepiolite or smectite and rare

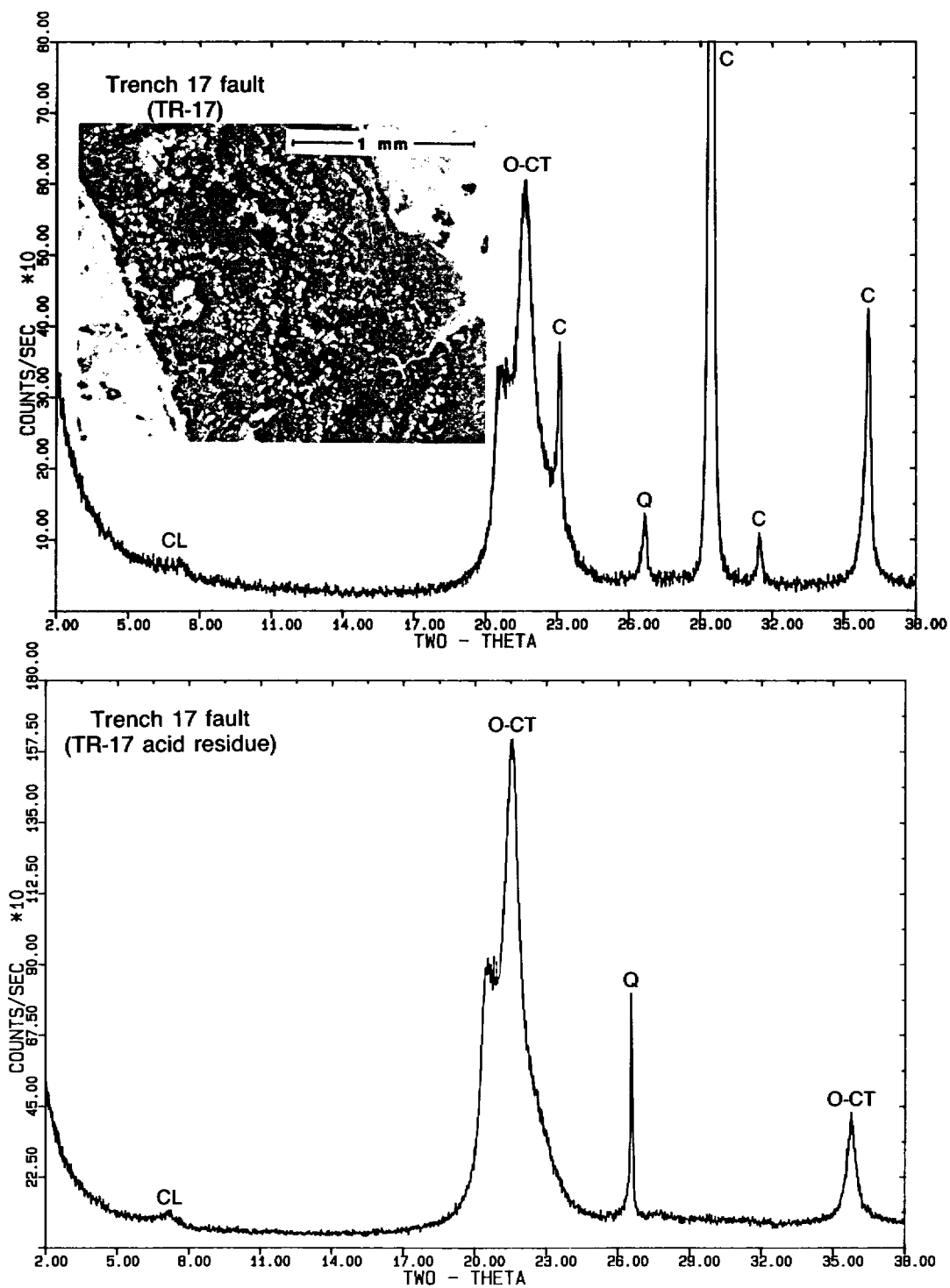


Fig. 10. XRD patterns of both a bulk sample (TR-17) and an acid-treated sample (TR17-1 acid residue) from Trench 17. Inset photomicrograph shows possible relic ooids(?) within the bulk sample. The diffraction peaks of calcite (C), opal-CT (O-CT), quartz (Q), and clay (CL) are labeled.

occurrences of opal-A. Opal-A appears to be restricted to young and fragile (relatively unfaulted?) accumulations of organically controlled silica deposition.

B. Hydrothermal Vein Deposits Near Yucca Mountain

Hydrothermal vein deposits are abundant throughout the silicic volcanic rocks of Nevada, often with associated mineralization. Where these veins approach the surface they may merge into warm-spring type deposits (Section C, below). Most descriptions of such systems emphasize the often associated deposits of economic minerals, primarily gold and silver (Sawkins 1984; Berger and Eimon 1983). The Tonopah district is one such locale, where quartz and quartz-calcite veins occur, which might be compared with the deposits in trenches near Yucca Mountain. Opalized zones can also be found near the surface in such systems (Berger and Eimon 1983); more will be said on this point in the discussion of warm-spring sinter deposits below. A major distinction between the Yucca Mountain fault deposits and the Tonopah-type deposits, however, is the association with sulfur and sulfide/sulfate minerals (alunite, pyrite, and base-metal sulfides) in the hydrothermal veins. One might argue that it would be more appropriate to examine barren hydrothermal deposits because there is so little economic potential at Yucca Mountain, but for the same reason that valuable hydrothermal deposits are so well known there is very little known about the barren ones. Fortunately, there have been several recent studies of hydrothermal alteration at Yucca Mountain itself, because Yucca Mountain is being considered as a potential site for high-level waste disposal.

What kind of hydrothermal alteration occurs at Yucca Mountain? Caporuscio et al. (1982) describe hydrothermal alteration assemblages at depths of 1000 m and more below the surface at the northern end of Yucca Mountain, in a region west and northwest of Trenches 14 and 17. This alteration is marked by the development of calcite pseudomorphs after volcanic feldspar phenocrysts, by illite, by calcite-quartz-barite veins, by pyrite, by fluorite, and by manganese minerals (e.g., todorokite). In a more recent study by Bish (in preparation), the data obtained from illite and smectite interstratifications have been used to estimate the temperatures of this hydrothermal alteration (temperatures from 100°C to greater than 275°C have been calculated, depending on depth and location within the hydrothermally altered zone). Moreover, the report by Bish (in preparation) presents some preliminary K/Ar age data from three illite samples of the hydrothermally altered zone that give consistent

ages of 11 Ma for the end of the hydrothermal alteration. Thus the hydrothermal features beneath the trenched faults near Yucca Mountain are deeper (1000 m), older (11 Ma), and mineralogically very different (common sulfide, sulfate, and manganese minerals) than deposits in the trenched faults.

There are also near-surface hydrothermal veins just 10 km to the north of Trenches 14 and 17. Most of these veins are quartz with minor accessory mineralization, but some of the veins contain opal. Figure 11 shows the XRD pattern of a quartz-opal-cryptomelane vein from the Calico Hills. In this sample, unlike the fault deposits, the opal is highly crystalline (opal-C; compare with Fig. 5). As in the hydrothermal alteration at depth beneath Yucca Mountain, manganese minerals are associated with the silica. The absence of sulfides and calcite in this near-surface vein suggests different fluids or different timing of emplacement as the fluids evolved, but both the deep and the shallow hydrothermal deposits near Yucca Mountain are unlike the calcite and opal-CT deposits, with opal-A and smectite or sepiolite, that occur near-surface in the faults close to Yucca Mountain.

C. Warm-Spring Deposits

Figure 1A shows the distribution of some active warm springs and some warm-spring sinter deposits in Nevada. One (Bailey Spring) is in Oasis Valley within 30 km of Yucca Mountain (Fig. 1B); the closest active springs with notable sinter deposits are far to the north, about 300 km from Yucca Mountain (Fig. 1A). In this section the efflorescence deposits in the valley floor at Oasis Valley, the sinter deposits around Steamboat and Brady Hot Springs, and a paleospring mound near Wahmonie (Fig. 1B) are described for comparison with the near-surface deposits in faults at Yucca Mountain.

1. Spring Deposits in Oasis Valley. Oasis Valley contains more than 20 springs with discharge temperatures ranging from 19°C to 36°C (White 1979). Many of the tuffs surrounding the valley have been altered, with alteration assemblages composed of kaolinite, alunite $[KAl_3(SO_4)_2(OH)_6]$, and opal-CT with lesser amounts of gypsum and calcite. It is not known whether this tuff alteration is related to present spring activity, but an analysis of the white to yellow-white efflorescence deposits in the valley includes one abundant sulfur-bearing phase: burkeite $[Na_6(CO_3)(SO_4)_2]$ occurs along with trona $[Na_2(CO_3):Na(HCO_3):2H_2O]$ and halite (Fig. 12). From the abundance of burkeite in the present-day efflorescence on the valley floor to the abundance of alunite in the past alteration of the tuffs, it is evident that the deposits produced in this system have always been strongly sulfur bearing. This type of

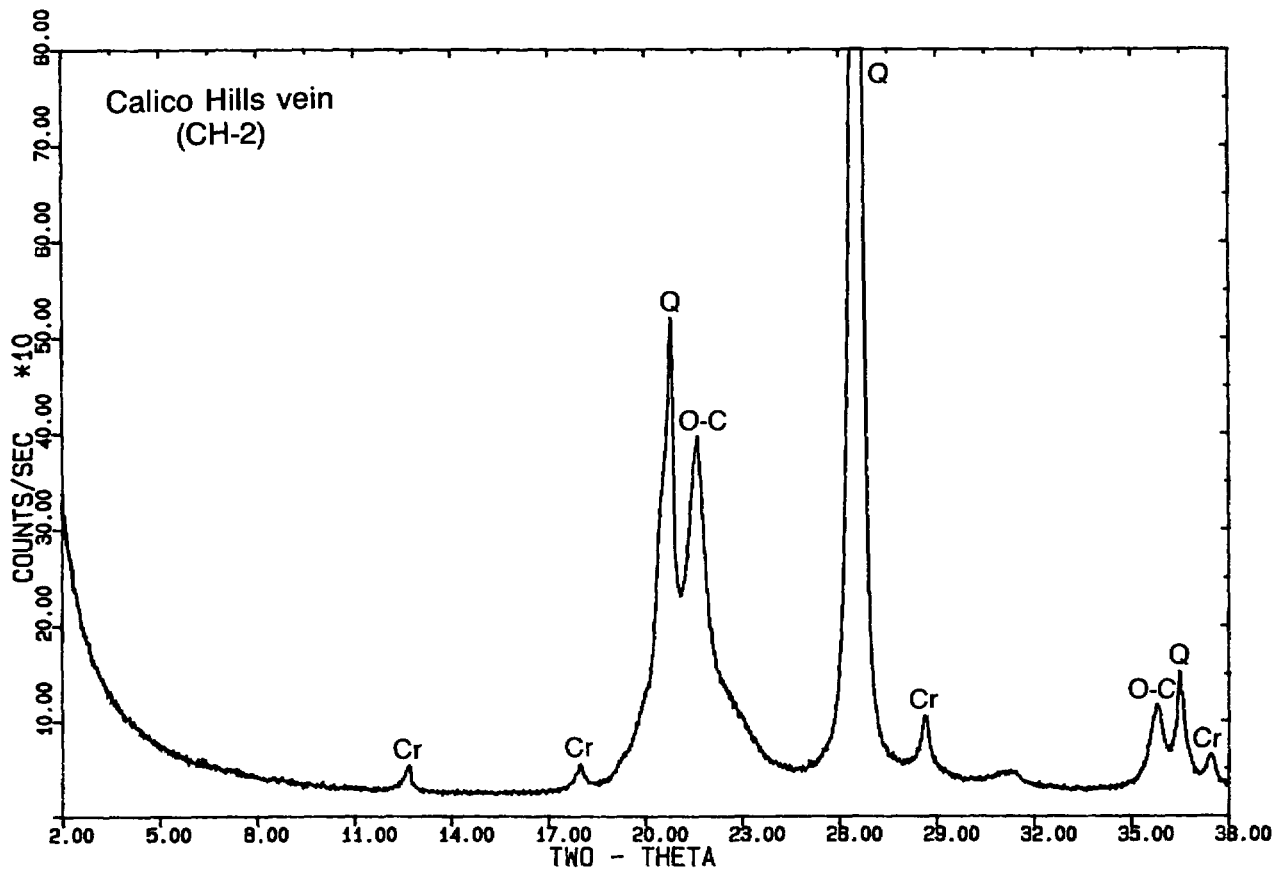


Fig. 11.

XRD pattern of a hydrothermal vein from the Calico Hills. The minerals labeled are quartz (Q), opal-C (O-C), and cryptomelane (Cr).

alteration and deposition is unlike the sulfur-free deposits in faults exposed near Yucca Mountain.

2. Warm-Spring Sinter Deposits. Warm-spring sinter deposits have been studied from the nearest localities (Horton 1964) at Steamboat Hot Springs and at Brady Hot Springs (also known as Springer's Hot Springs). These sinter deposits are characterized by localized accumulations of almost pure opal-A (Fig. 13), along with sulfur or sulfur-containing minerals such as gypsum and alunite. The association with sulfur is evident even in the most purely opaline sinter materials, where trace-fossil tubules contain small residues of pyrite (inset photomicrograph, Fig. 13). At Sou Hot Springs (Fig. 1) the altered tuff also contains gypsum. Further studies are planned of these and other sinter deposits of the region, but the data available so far are consistent in demonstrating the ubiquitous presence of sulfur that is unlike the calcite-silica deposits in the faults exposed around Yucca Mountain.

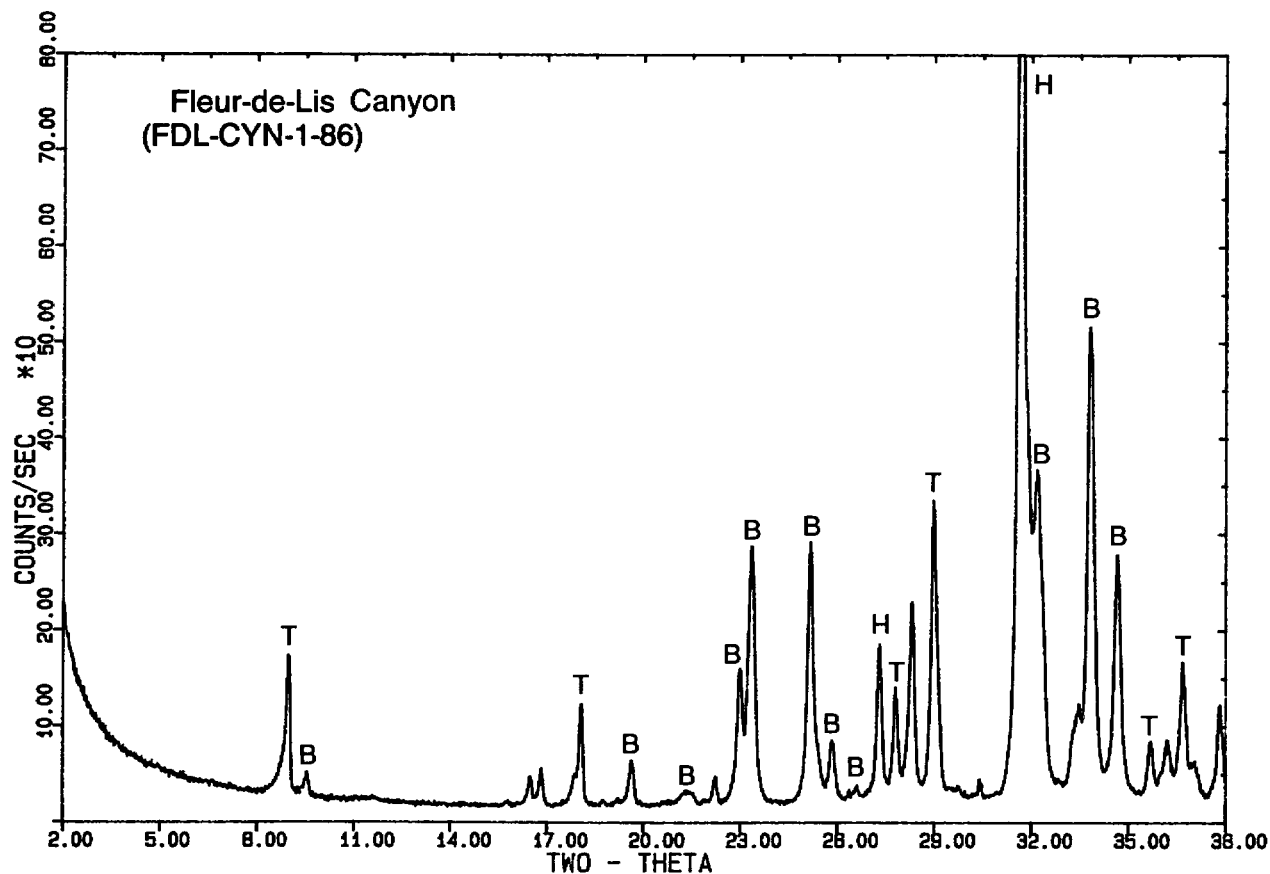


Fig. 12.

XRD pattern of spring efflorescence from Oasis Valley. The diffraction peaks labeled are halite (H), burkeite (B), and trona (T).

In the discussion of hydrothermal veins (Section B), an important feature of the hydrothermal vein deposits around Tonopah was their association with sulfur-bearing minerals such as alunite. This association is evidence that the sulfur-silica systems found around the sinter deposits in west-central Nevada mirror the near-surface hydrothermal vein deposits of the same region. The relation between warm-spring deposits and the formation of shallow mineralized veins has been known at Steamboat Hot Springs for over a century (LeConte 1883). Thus both the hydrothermal veins and the surface sinter might be considered as essentially a single depositional system with depth gradations, such as Ross et al. (1982) describe at Roosevelt Hot Springs in Utah (in which sulfur minerals are also important associates with silica sinter).

This comparison of the fault deposits at Yucca Mountain with Nevada's sinter deposits begs the question of what a sinter deposit would look like in a sulfur-poor warm-spring system. For an interim answer, petrographic and XRD

data have been examined from an extensive siliceous sinter area at San Ignacio in Honduras. Although far from Nevada, this sinter also overlies an area of crustal extension. More importantly, this system is relatively sulfur-free. The sinter deposits here are petrographically different from the Nevada sinters; where the Nevada sinters contain laminated botryoidal opal with a few trace fossil remains (photomicrograph in Fig. 13), the San Ignacio sinters consist of cemented masses of opaline plant fossils (Table III). In both types of sinter deposits, however, the opal is opal-A. Warm-spring sinters are characterized by primary deposition or organic-debris cementation with amorphous opal (opal-A). With time the opal-A sinters alter to β -cristobalite, α -cristobalite, chalcedony, and then to quartz (D. White, oral communication, August 1987). Silica sinters do not alter to opal-CT in a manner analogous to the well-studied diagenetic sequence in deep-sea oozes and in siliceous sediments (Kano 1983; Kastner et al. 1977; Williams et al. 1985). The opal-A in silica sinters instead develops cristobalite but not tridymite stacking (D. White, oral communication, August 1987). Other near-surface systems with hot circulating water could transform directly from opal-A to quartz (Oehler 1976). The complications of likely disequilibrium and impure systems (Williams et al. 1985) make theoretical treatment of these transitions largely impractical. More field data and documentation on the alteration of aging opal-A from sinter deposits are needed. However, the lack of opal-CT in sinter deposits is another feature that makes them different from the deposits in faults around Yucca Mountain.

3. The Paleospring Mound at Wahmonie. Although the only active warm springs close to Yucca Mountain are in Oasis Valley, there is a paleospring mound on the Nevada Test Site above Wahmonie, 28 km east of Yucca Mountain (Fig. 1B). This spring mound consists of almost pure gypsum with minor calcite (Fig. 14) and appears to represent deposits from an old hot-water discharge centered in the Wahmonie ore district, which was once mined for gold, silver, and copper (Bell and Larson 1982). As at Tonopah, this hydrothermal system combines precious metals with sulfur-bearing mineralogy. Silica sinter, however, does not occur at Wahmonie. In its abundance of gypsum and lack of silica, the paleospring mound at Wahmonie is quite different from the fault-related calcite-silica deposits near Yucca Mountain.

D. Cold Springs or Seeps, and Playa Deposits

Several active cold springs or seeps occur within a few tens of kilometers of Yucca Mountain. The springs of Oasis Valley include warm discharges and

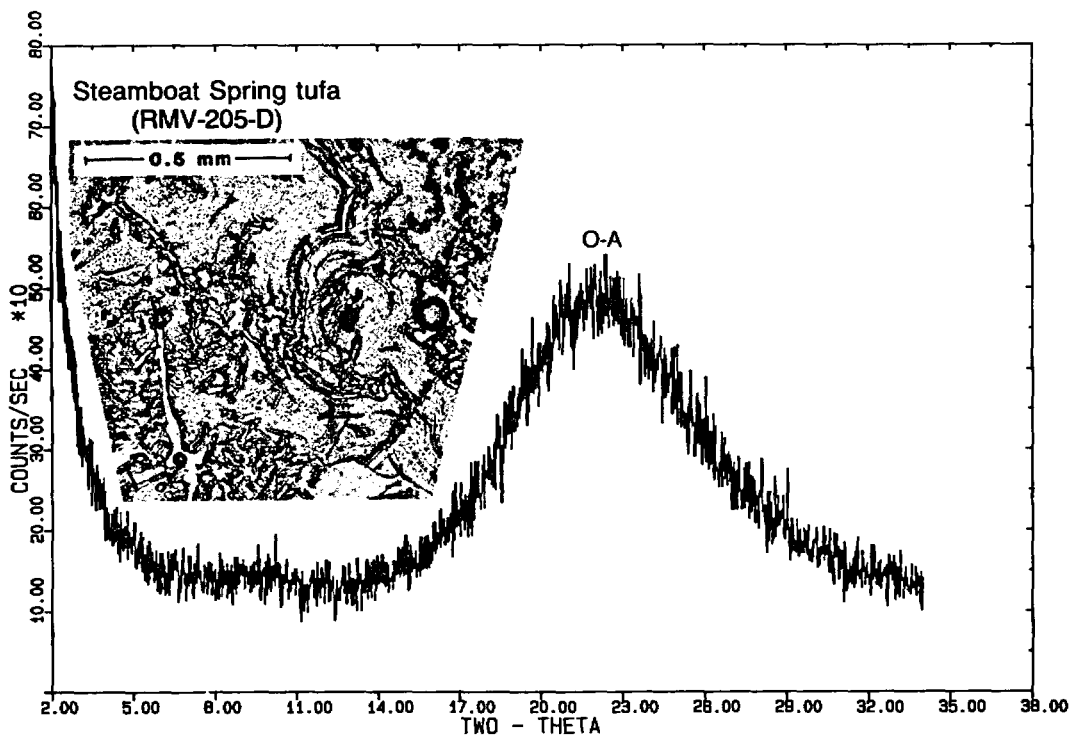
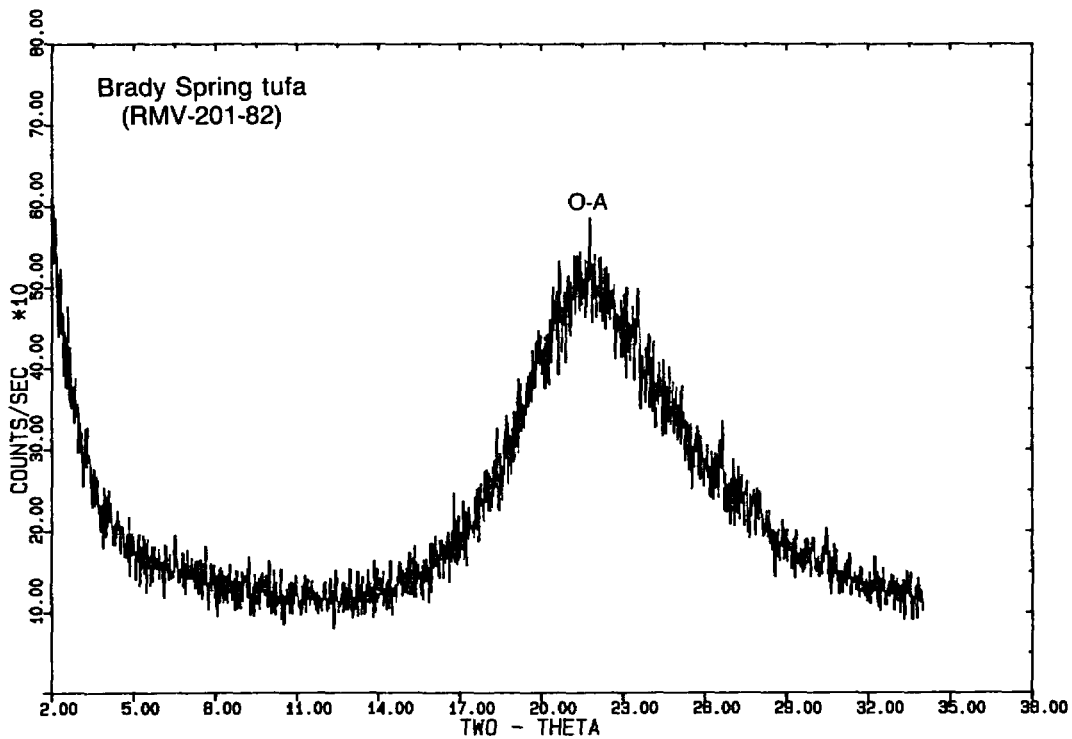


Fig. 13.
XRD patterns of opal-A sinter from the warm springs at Brady (RMV-201-82) and at Steamboat Hot Springs (RMV-205-D). Inset photomicrograph shows tubules of organic origin containing small pyrite crystals in the opal-A of sample RMV-205-D.

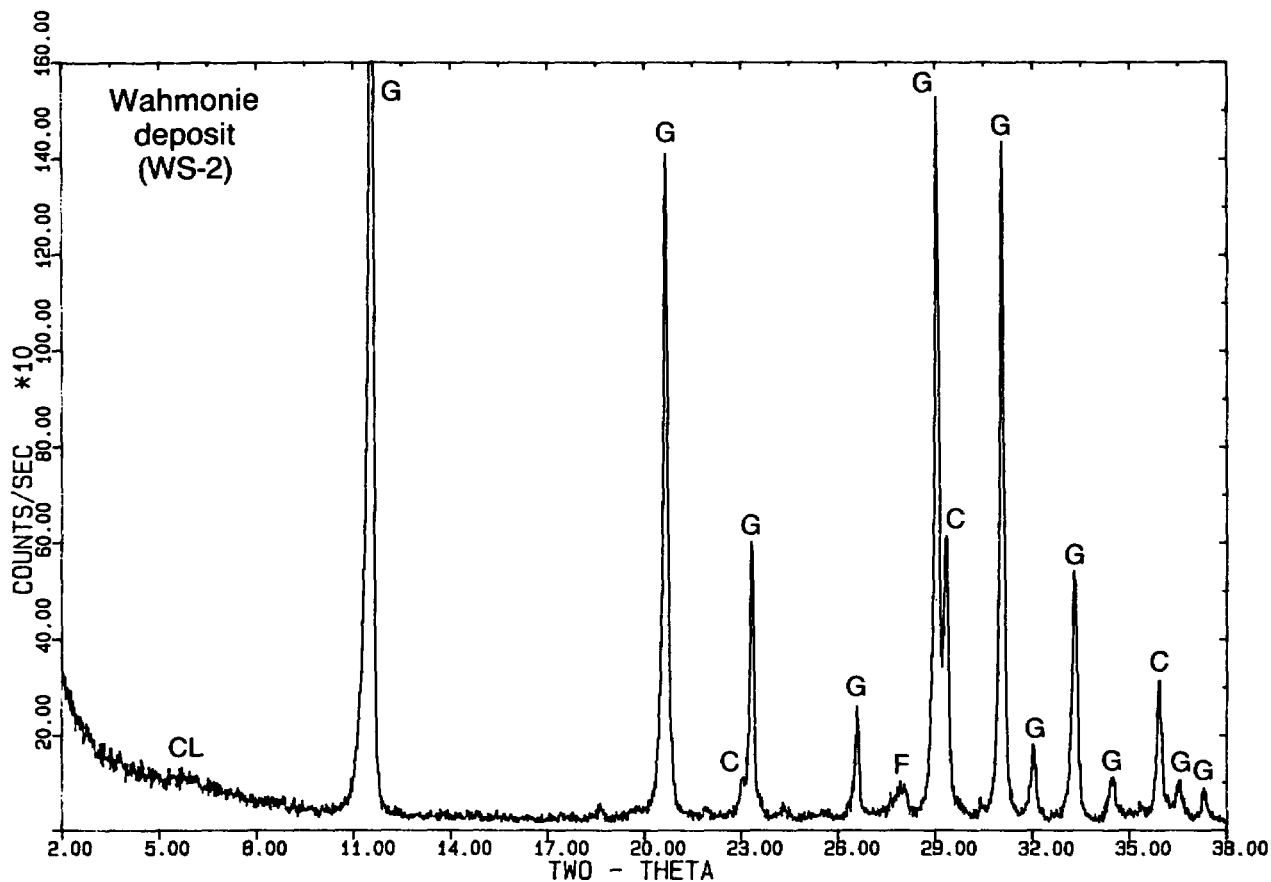


Fig. 14.

Gypsum (G) of the paleospring deposit near Wahmonie, with minor amounts of calcite (C) and clay (CL).

valley-floor efflorescences that are described in Section C above. The springs of Death Valley, with their carbonate deposits and the associated carbonate deposits at Devil's Hole and along the eastern edge of the Amargosa Valley, are described by Winograd et al. (1985). A complete set of samples for these deposits is not yet available, but one sample of the calcite deposit at Nevares spring has been studied. The sample studied is dense and buff colored, superficially similar to the dense lenticles that are found in the fault at Trench 14 (e.g., sample T14-F described in Section III). However, petrographic and XRD analyses show that the Nevares sample consists of almost pure calcite occurring as masses of euhedral microspar crystals with scalenohedral habit (Fig. 15). These crystals are of intermediate-Mg calcite (Milliman 1974) rather than low-Mg calcite as in Trench 14 and at the tufa deposit southwest of Moapa (described below). This distinction, however, is based on a small difference in magnesium content. The absence of any authigenic silica phase is more significant and makes this deposit very different from the calcite-silica deposits in faults around Yucca Mountain.

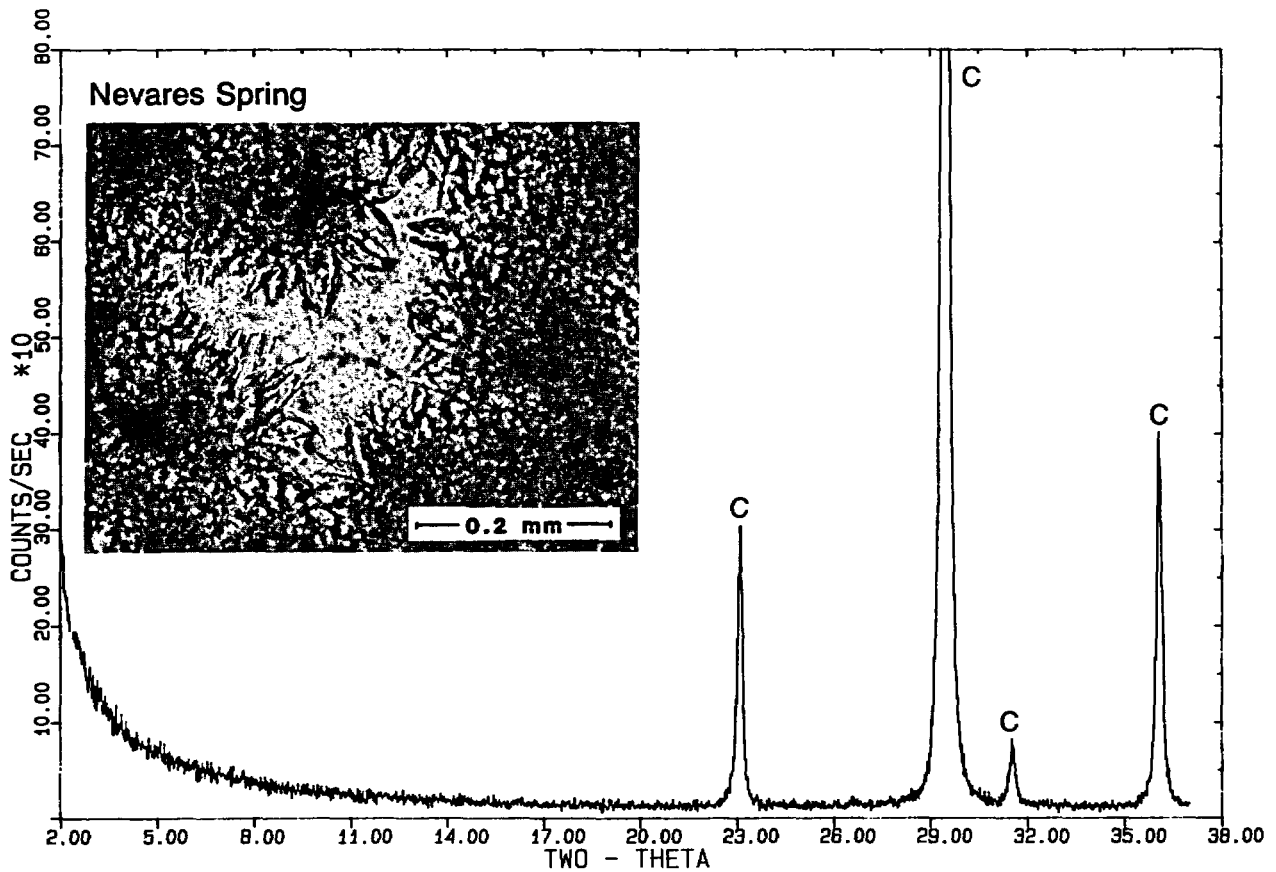


Fig. 15.

Calcite (C) of the dense microspar tufa from Nevares. Inset photomicrograph shows scalenohedral habit of the calcite microspar.

Several springs occur on the Nevada Test Site not far from Yucca Mountain. Topopah Spring contains no deposits except for some very thin rinds of calcite on nearby boulders and cobbles; these deposits are of questionable origin because they are as likely to be caliche as deposits from the spring. Cane Spring has small calcite mounds and pedestals of less than 1-mm diameter underlying live algae near the point of spring discharge. These deposits at Cane Spring are of pure calcite. Both Topopah and Cane Springs issue from tuff, but a small seep that issues from a thrust separating Mississippian Eleana argillite from overlying quartzite is described by Jones (1983) and has a deposit of calcite with abundant sepiolite. This seep, at the eastern flank of the Eleana range, is shown in Fig. 7. The sepiolite-calcite assemblage at the Eleana locality is closer in resemblance to the deposits in faults around Yucca Mountain, but even the Eleana seep deposit lacks the abundant opal of the faults at Yucca Mountain. Sepiolite from this locality is characterized by a highest-intensity peak at 12.6 Å and distinguished from palygorskite by a peak at 2.68 Å (Jones 1983, his Fig. 2). Sepiolite from Trench 14 (Fig. 6) differs

by having comparable diffraction maxima at $7.2^\circ 2\theta$ (12.3 \AA) and $34.86^\circ 2\theta$ (2.57 \AA). There are not yet enough data to indicate whether the smaller lattice spacings at Trench 14 are significant.

1. Paleospring Deposits South of Yucca Mountain? Szabo et al. (1981) describe two localities, with their identifying numbers 106 and 199 (Fig. 1B), as being a possible seep deposit of about 78 000 year age (locality 106) and a possible spring deposit of about 30 000 year age (locality 199). Locality 106 appears to be fault related and has field relations (deposit draped over a slope gradient from a subhorizontal surface into a fault) similar to those exposed in Trench 14. Locality 199 is poorly exposed. Both of these localities will require excavation and mapping before samples are collected for mineralogic comparison with other localities. There are not yet sufficient data to determine whether these deposits might be associated with warm-spring, cold-spring, seep, or soil-process origins.

2. Paleospring Deposit Near Moapa. A paleospring travertine deposit occurs in Dry Lake Valley southwest of Moapa (Fig. 1B). Estimates of paleotemperature have not been made in this study, but the preservation of triangular casts of bull rushes near the paleospring source indicate that temperatures were not so high as to leave the mound barren of such plants. Present spring discharge in the Moapa area is about 32°C (Garside and Schilling 1979), but no direct connection between this active discharge and the deposits in Dry Lake Valley is known. The description of this spring travertine deposit is provisionally included with cold-spring deposits.

The remains of the spring orifice contain numerous tubular structures with walls constructed of concentric rings of small (0.02-0.06 mm) radially arranged calcite crystals (Fig. 16). The tubes themselves are a few centimeters in diameter. Central openings in the tubes were originally up to 1 cm in diameter but are now almost plugged with detrital mineral grains (quartz, with lesser amounts of microcline, plagioclase, pyroxene, biotite, amphibole, and altered lithic fragments) and with calcite ooids of 0.05-0.25-mm diameter. XRD analysis shows the tube walls to be composed of almost pure calcite (Fig. 17); electron microprobe analysis (Table II) shows that the calcite is low-Mg, comparable to the calcite in Trench 14. The greatest difference between this deposit and that at Trench 14 (Section A, above) is the absence of authigenic silica. At this paleospring travertine deposit, however, there is an outflow facies that extends for several tens of meters from the central source. It is appropriate to examine how the mineralogy and petrography of the travertine change away

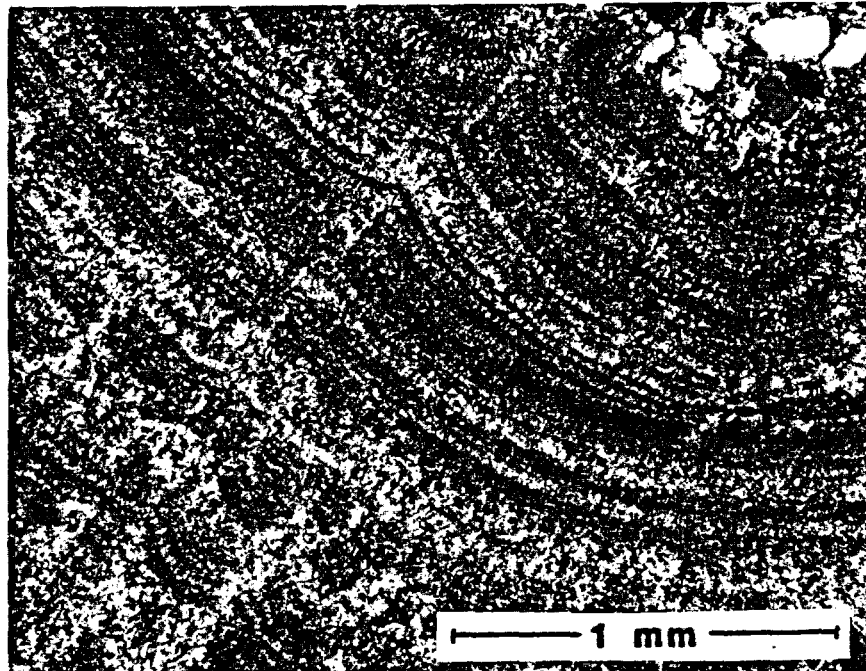


Fig. 16.

Photomicrograph of laminated calcite growth in discharge tubules of the tufa mound southwest of Moapa (sample MO-1).

from the source, particularly where surface weathering and soil formation have occurred.

Figure 17 compares the XRD pattern for the pure calcite of the travertine source tubules (MO-1) with banded travertine 0.5 m deep within the outflow facies (MO-2) and with travertine at the surface of the outflow facies (MO-3). Sample MO-2 contains a smectite not found in the spring source; sample MO-3 contains more of this smectite, suggesting that clay formation is part of the transition from travertine to soil in the flat outflow sheet. It is important to note that authigenic silica does not form as part of the alteration process. The quartz in samples MO-1, MO-2, and MO-3 (Fig. 17) is detrital and with other detrital minerals forms nuclei for ooids. Both samples MO-2 and MO-3 contain the same detrital minerals as found in MO-1. These samples are characterized by abundant ooids. Small simple ooids of 0.05 mm occur, usually without cores of detrital minerals. Ooids of 0.3-0.4-mm diameter are abundant; many have detrital mineral cores. Sample MO-2 also contains complex ooids up to 1 mm across, some of which are formed by coalescence of several smaller ooids. Several bands of ooids in MO-2 appear to be matrix supported by micrite in the

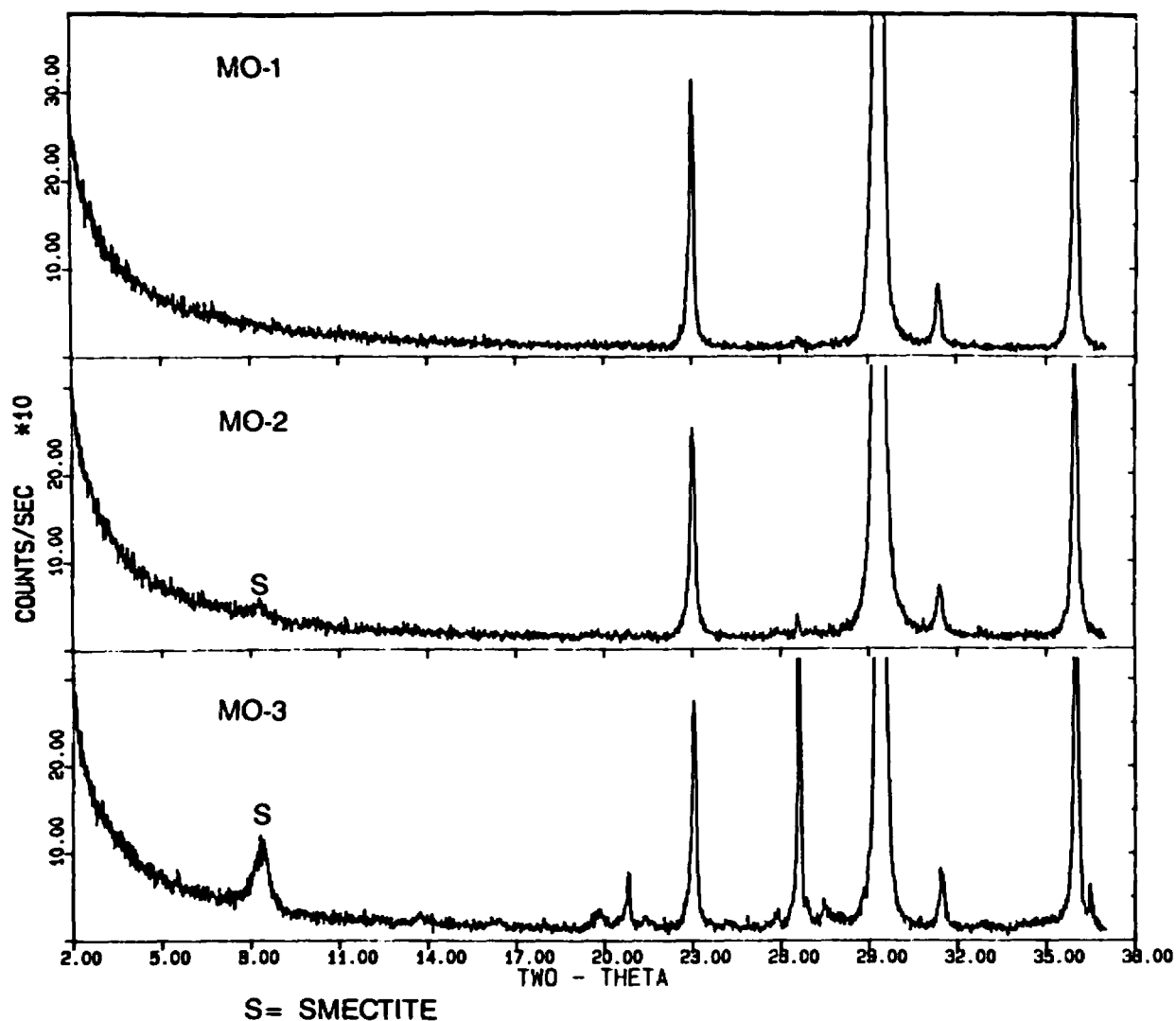


Fig. 17.

XRD patterns compared for a discharge tufa mound southwest of Moapa (MO-1), for a sample 0.5 m deep in the outflow deposit from the tufa mound (MO-2) and for the surface of the outflow deposit immediately above sample MO-2 (MO-3). The progression from spring tufa to weathered deposit results in increased smectite (S) content. Quartz (Q) is detrital and forms one of the common nuclei for calcite ooids.

upper few millimeters but grain supported (ooids compacted together) in the bottom of the band. Recrystallization of ooids is common, particularly in MO-3 where voids are lined by small calcite spar crystals of up to 0.5 mm. The abundance of ooids is greater than in the deposits of Trench 14, but the presence or absence of ooid forms is not distinctive between the two environments. The greatest difference between the deposits within faults and the Moapa spring locality is the absence of opal in all facies of the spring deposit.

3. Playa and Playa/Seep Deposits of the Amargosa Valley. Deposits of the Amargosa Playa (Fig. 7) have been described in detail by Papke (1972), Post (1978), Khoury et al. (1982), Jones (1983), and Hay et al. (1986). These descriptions have concentrated on the sepiolite found in this playa, and all have concluded that sepiolite can precipitate directly from solution in such an environment. Khoury et al. (1982) conclude that sepiolite saturation can occur in the local groundwater after about 10% evaporation. Within this playa deposit there are beds of essentially pure (80%) sepiolite with no other authigenic minerals, bounded by beds of an authigenic smectite-sepiolite-dolomite-calcite assemblage (Khoury et al. 1982). Paleospring mounds occur southwest of the Amargosa Playa in the Hectorite-Whiting pit along the Amargosa River (Fig. 1B); these deposits contain the assemblage calcite-smectite-chalcedony-quartz. These Amargosa River spring mounds described by Khoury et al. are more similar to the deposits in faults around Yucca Mountain than are the playa deposits, although the silica in the spring mounds is relatively minor and consists of a late fracture filling by quartz rather than by opal.

The complex groundwater alteration of playa deposits described by Hay et al. (1986) along Carson Slough (Fig. 1B) is the closest playa/seep approximation of the mineralogy precipitated in faults around Yucca Mountain. At Carson Slough the original playa deposits of limestone, dolomite, and clays (with local phillipsite and K-feldspar) have been replaced by opal-CT, chalcedony, and quartz from siliceous groundwaters. Distinct from the Yucca Mountain fault deposits is the transformation of opal to quartz and the two-stage separation of early carbonate and later silica deposition, without co-precipitation. Nevertheless, the partial similarity between this playa/seep deposit and the deposits in faults at Yucca Mountain is of interest and will be reviewed in the summary and conclusions (Section V).

E. Soil Deposits

Post (1978) describes caliche in an alluvial terrace north of Las Vegas as being somewhat similar to the Amargosa Playa deposit: calcite at the top, with sepiolite-dolomite at greater depth. In general, however, dolomite does not form in soils of the region and sepiolite occurs with calcite instead (Hay and Wiggins 1980; Jones 1983). A further characteristic of soils is the occurrence of opal, often occurring as a coating on ooid or pellet structures that are common among the calcretes (Hay and Wiggins 1980). Hay and Wiggins report that opal in the calcrete of Kyle Canyon, in the Spring Mountains west of Las Vegas (Fig. 1B), occurs as cement, veinlets, and ooid coatings of opal-A and in

chertlike layers and nodules of opal-CT. Thus, as in the fault-related deposits described in Section III, both opal-A and opal-CT are present, although the relative abundance and the textural distributions are different: the fault-related deposits consist predominantly of ooid coatings and relatively pure laminae of opal-CT, with opal-A restricted to occurrences in which organic structures are preserved.

Hay and Wiggins (1980) cite evidence for the replacement of sepiolite and calcite by silica. They attribute this to a change in water chemistry, either due to short-term increased rainfall or to the long-term increase in Pleistocene vegetation leading to higher pCO_2 and lower pH in the vadose zone. These conditions would be sufficient to account for the cessation of carbonate deposition, although the conditions leading to opal deposition are not known and may include a combination of the principal factors of organic fixation, evaporation, temperature, and local pH variations (Summerfield 1983) as well as being dependent on the relative purity of local fluids (Williams et al. 1985). The problems of trying to unravel which of these parameters were operative are multiplied by the consideration that "microsite" deposition was probable (Chadwick and Hendricks 1985), with a multitude of small isolated environments that were not necessarily all evolving in the same way.

The assemblage calcite-opal-sepiolite is found in soils of the region, but the most relevant comparison to the deposits in Trench 14 will be of soils from the immediate environment. It is important to emphasize that soil mineralogy can be quite variable on a local scale; Jones (1983), for instance, describes the regional transition from palygorskite at Mormon Mesa (Fig. 1) to sepiolite in samples around Yucca Mountain. Jones also found variation in soil deposits over a much smaller range around Yucca Mountain. For example, he found that calcic soils immediately west of Trench 14 (Fig. 7) contain no sepiolite or only traces of material that might be tentatively identified as chain-structure clay, whereas there is well-formed sepiolite in some (but not all) of the calcic soils in Jackass Flat and in Crater Flat. A more detailed study of soils in the area around Yucca Mountain is being pursued by E. Taylor (USGS); Fig. 18 shows the XRD patterns from one of the carbonate-plugged horizons in one of the oldest soils based on the soil geochronology developed by Taylor (oral communication, January 1986), following the work of Hoover et al. (1981). The XRD pattern of the bulk sample (Fig. 18) is complicated somewhat by detrital minerals, but the pattern of the clay-mineral separate is clearly of illite rather than that of a chain-silicate clay such as sepiolite. This illite is

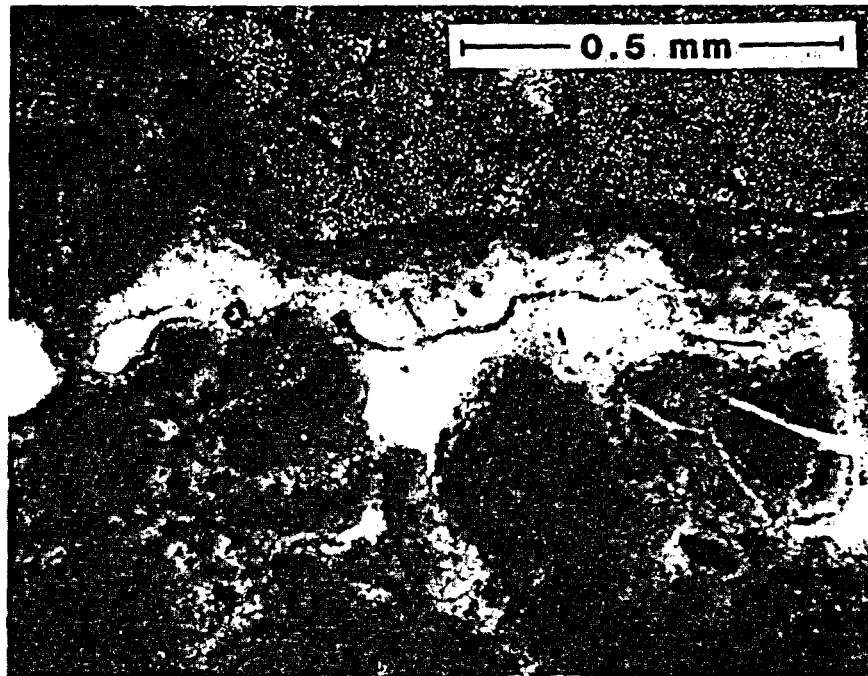


Fig. 18.

Photomicrograph of clear, botryoidal opal (opal-CT?) concentrated in the tops of voids between ooids and below a pebble in soil sample YW-2.

probably detrital rather than neofomed. In thin section, calcareous ooids (0.3-1.0-mm diameter) are common as in the fault-filling samples of Trench 14, but opal is relatively rare and occurs in the topsides of open voids between ooids (inset photo in Fig. 18) and coating the bottoms of some pebbles. Opal was not abundant enough in YW-2 for XRD determination of which structure type is present, and the development of discrete opaline layers or bands as in Trench 14 is not seen in this or in other terrace-forming soils of the area (E. Taylor, oral communication, January 1986). A separate split of this sample (YW-2,R) was analyzed by XRD to determine the opal types, and the probable presence of both opal-A and opal-CT was found. Even in this old soil with extensive silica deposition, there is not as much silica as in the nearby fault deposits.

F. Calcite-Silica Deposits in Aeolian Sequences

Aeolian sands occur in several areas around Yucca Mountain. One of the most prominent areas of aeolian deposition is around Busted Butte and along the western flank of Fran Ridge (Fig. 1C); in this area the sand deposits are several meters to several tens of meters thick and record a complex series of

deflation and deposition events that can cumulatively form "sand ramps" around the tuff buttes and ridges (J. Whitney, USGS, oral communication, February 1986). The upper portions of the sand ramps in this area commonly contain a slope-parallel calcite-silica deposit or a series of calcite-silica deposits that are approximately slope-parallel. Faults that cross upward through the sand ramps contain similar deposits (Fig. 19).

Figure 20 compares samples from a slope-parallel deposit on the flank of Fran Ridge (FR-6), a slope-parallel deposit from the northern flank of Busted Butte (BB-1), a near-surface fault filling from the western flank of Busted Butte (BB-2) and the slope-parallel deposit immediately above it (BB-3), and a clay-mineral separate (BB-5) from the surface sand immediately above the BB-3 deposit. All of the deposits, either along the sand ramp slopes or in the faults, consist predominantly of opal-CT and calcite, plus a clay mineral or clay minerals. The crystallinity of the opal may vary greatly between closely related samples; note that the slope-parallel deposit BB-3 has a much sharper opal-CT diffraction maximum at about $22^\circ 2\theta$ than the immediately underlying fault-filling sample BB-2.

Samples BB-3 and BB-2 were collected to examine the differences between slope-parallel deposits and the underlying fault fillings. In addition to the difference in opal crystallinity, the calcite-opal intergrowth textures differ in these samples. The slope-parallel deposit, BB-3, contains elongate cellular structures that appear to be fossilized plant remains oriented parallel to the deposit foliation (Fig. 21). Vegetation of the area is dominated by the genus *Larrea* (creosote bush) but includes mixed *Lycium* (boxthorn) and other plants (US DOE 1986). The fossilized remnants have not been correlated with a specific species but represent a vascular plant in which the cell walls have been replaced by very fine-grained calcite and silica, and the cell interiors are filled by relatively clear opal. No such structures are found in the underlying fault filling (BB-2), and we infer that the in situ deposition of discrete opal during plant fossilization in the slope-parallel deposits formed a more ordered opal polytype than did the mixed calcite-silica intergrowths within the underlying fault.

The clay minerals in these deposits will not be described in detail in this report. Studies of the clay separates are still in progress and indicate a complex series of poorly crystallized smectites and possible chain-silicate clays. Figure 20 shows the XRD pattern of the very poorly crystallized smectite fraction of sample BB-5, from the sand overlying the slope-parallel

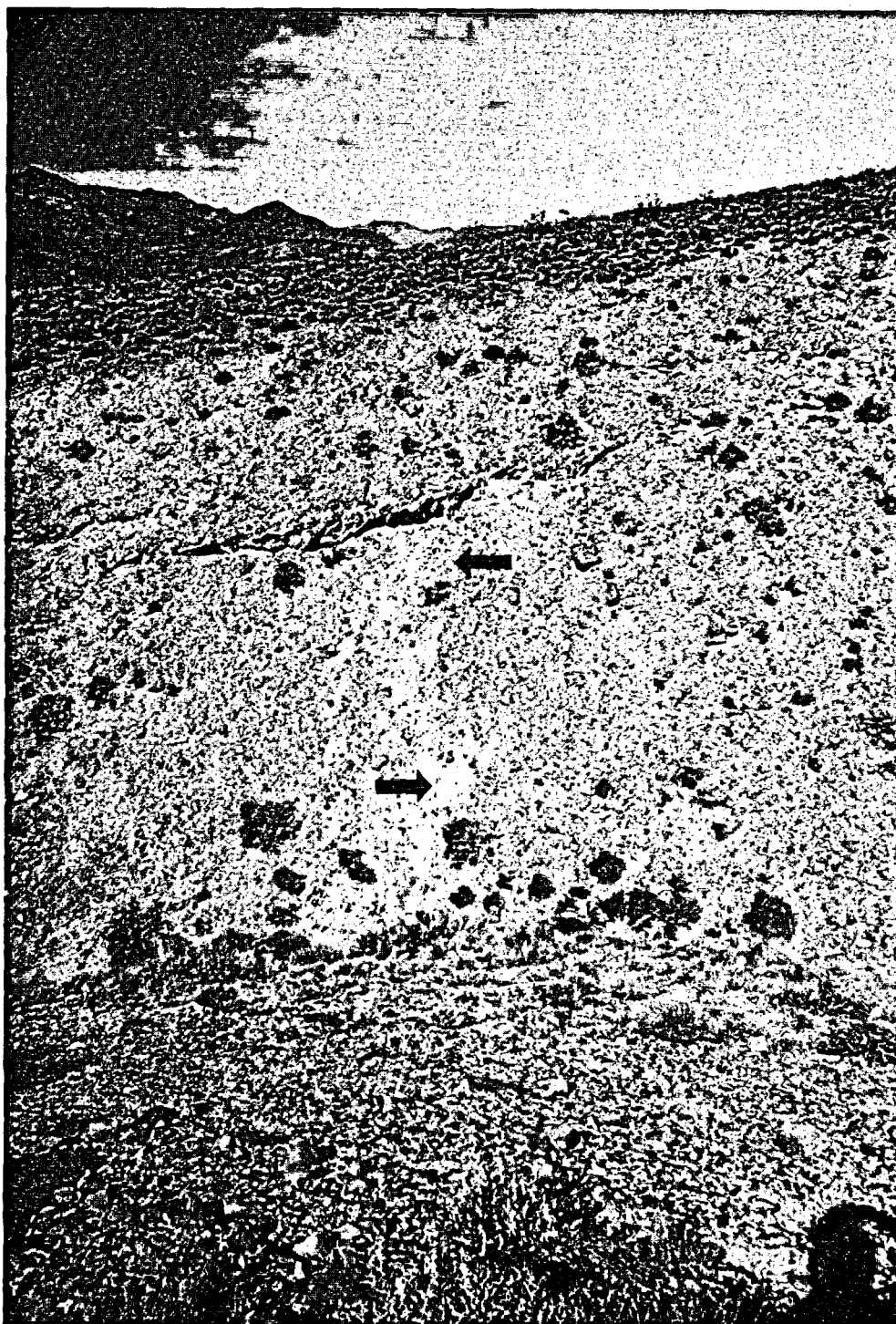


Fig. 19.
Photograph of slope-parallel calcite-silica deposit in a sand ramp on the western flank of Busted Butte. Arrows mark a thin fault filling of calcite and silica that crosses the slope-parallel deposit. Depth from the ridge crest to the bottom of the ravine is 7.5 m.

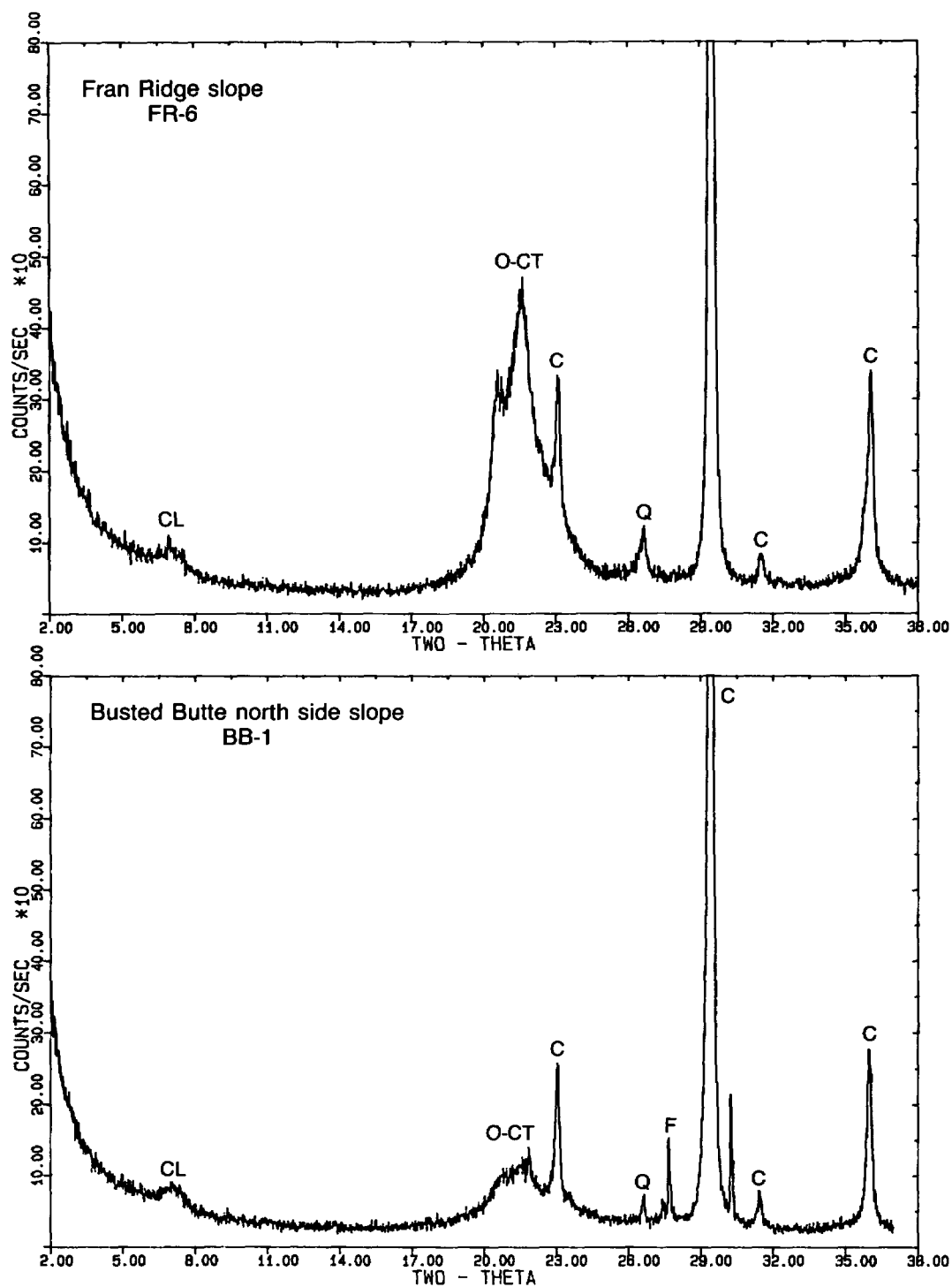


Fig. 20.

XRD patterns comparing slope-parallel calcite-silica deposits at Fran Ridge (FR-6) and at Busted Butte (BB-1 and BB-3), a fault-filling calcite-silica deposit in the sand ramp at Busted Butte (BB-2), and standard room-temperature and glycolated smectite samples (BB-5 RT and glyc.) from the sand overlying sample BB-3. Minerals indicated are calcite (C), opal-CT (O-CT), clays (CL), smectite (Sm), and detrital quartz (Q) and feldspar (F).

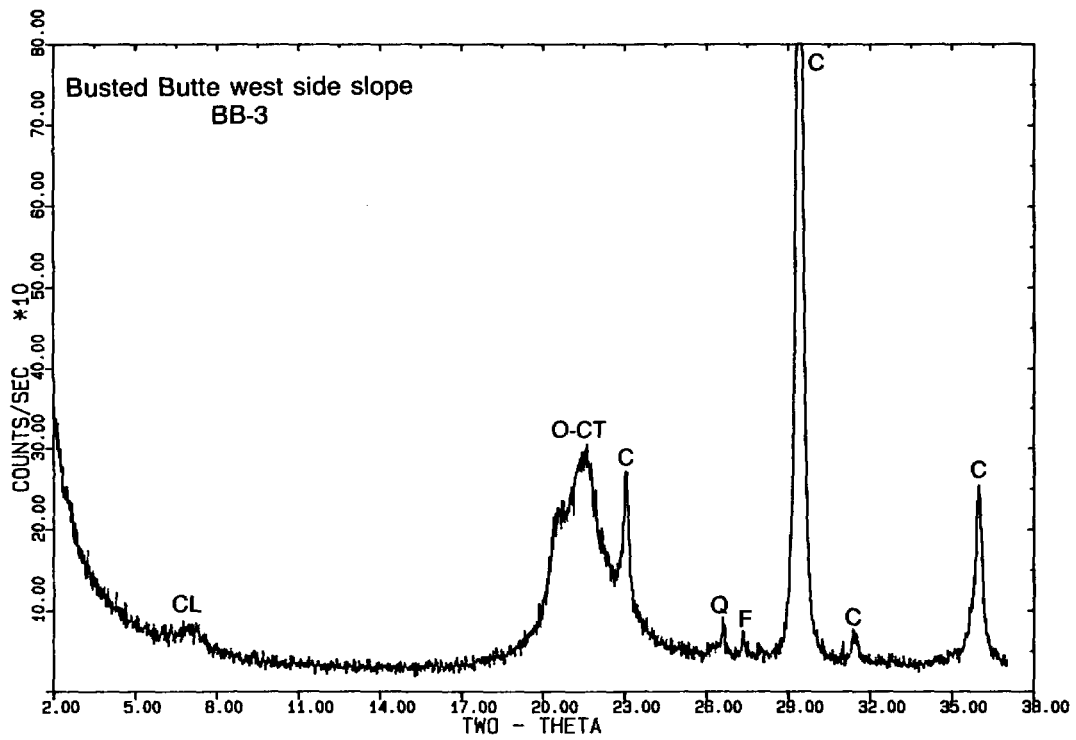
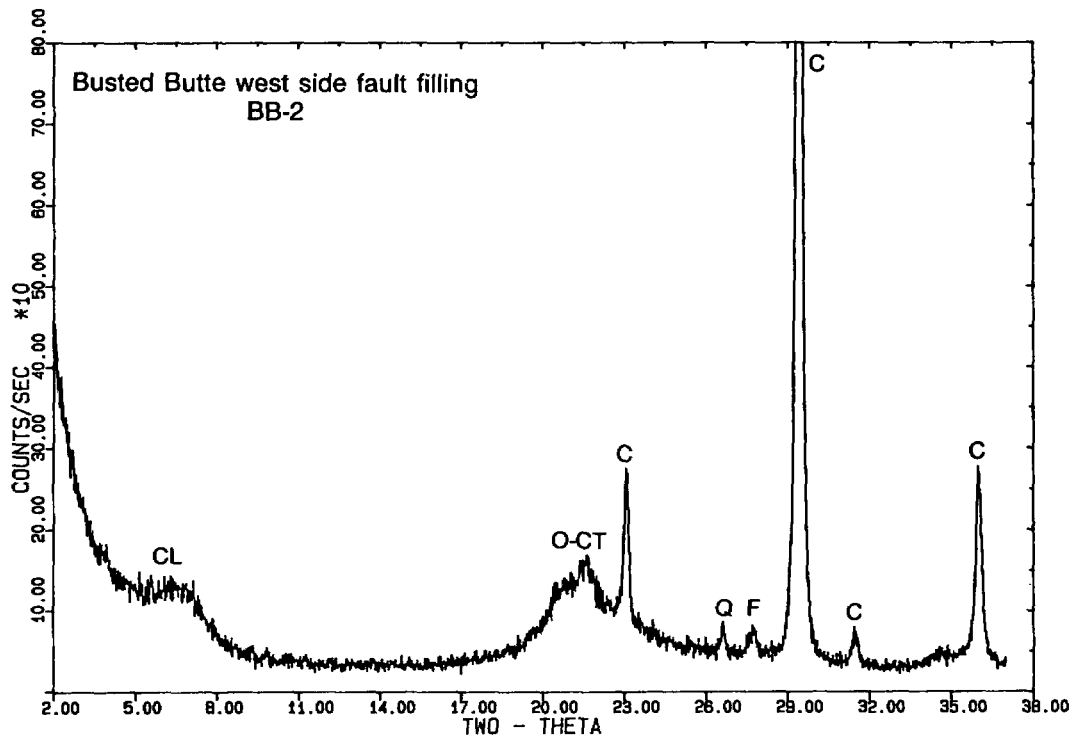


Fig. 20. (cont)

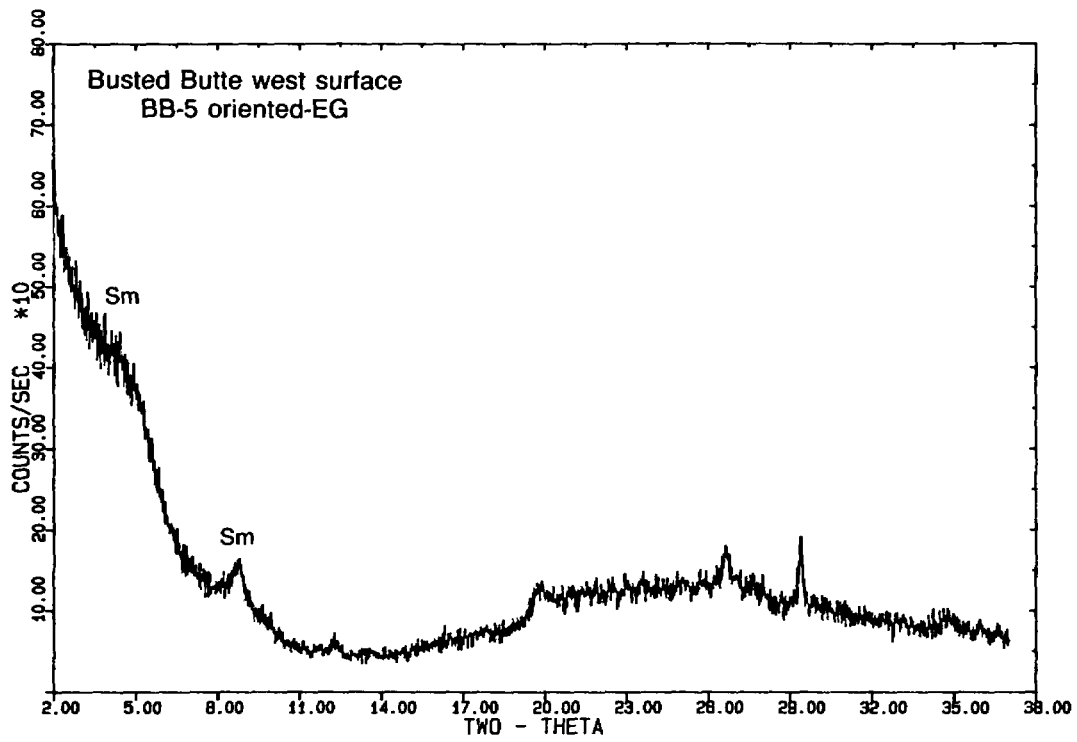
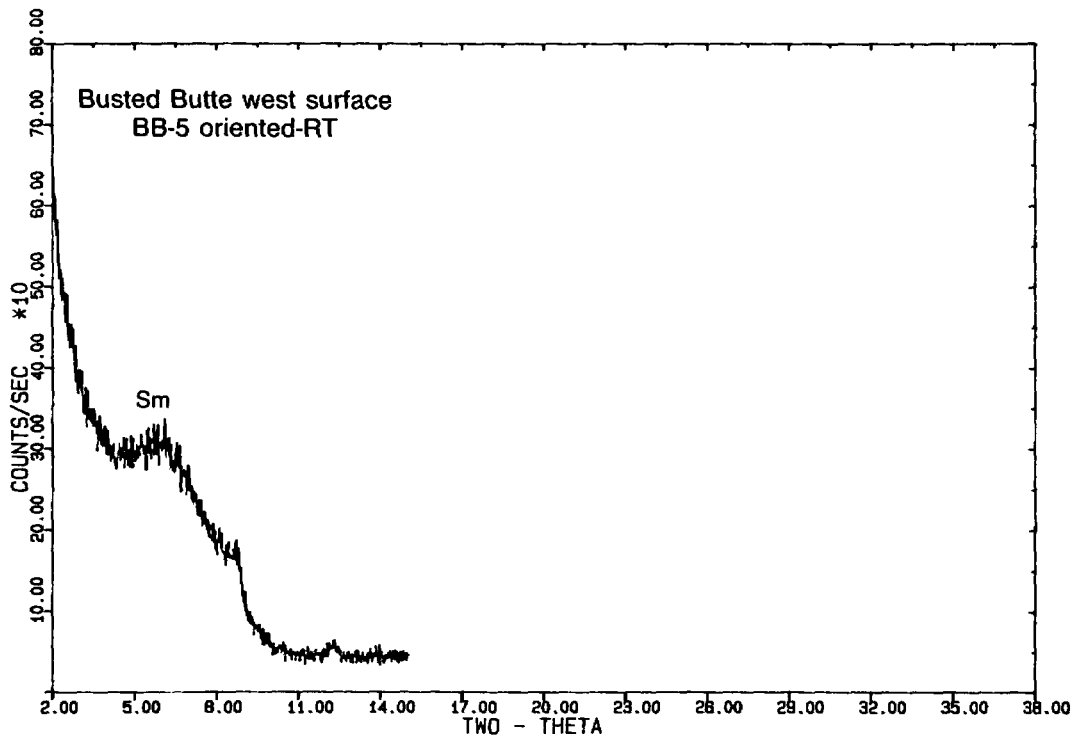


Fig. 20. (cont)

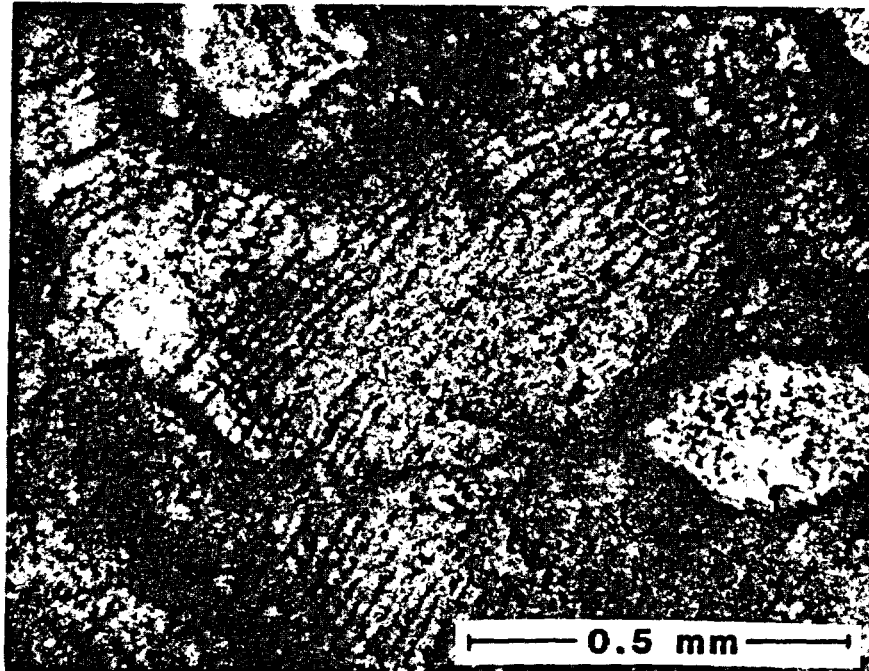


Fig. 21.

Photomicrograph of fossil plant materials in sample BB-3. The cell walls are replaced by calcite and opal-CT; the cell interiors are filled by opal-CT.

deposit BB-3. The major features of these deposits, however, have to do with the abundance and distribution of calcite and opal.

In the deposits at both Busted Butte and Fran Ridge, there are segregated laminae of opal-CT up to a millimeter wide and a centimeter long. Although smaller than the comparable laminae within the fault at Trench 14, the development of discrete opal-CT laminae is consistent in both the sand ramp deposits and the fault fillings. Calcite and opal-CT in the matrices of these deposits contain some ooids with diameters up to 1.0 mm; the concentric rings of these ooids are often separated by open intervals within which opal has been deposited. Clast-rich bands are cemented by a calcite-rich matrix that separates the clasts; many of the clasts have coatings of very fine-grained calcite-silica that may represent the initiation of ooid formation around foreign nuclei. Similar coatings are found around mineral and lithic fragments in the sandy fracture fillings within the fault at Trench 14. The clast populations in the sand ramps and in Trench 14 are extremely varied, including sand-size fragments of quartz, plagioclase, potassium feldspar, pyroxene, amphibole, olivine, magnetite, "quench"-texture remnants from basaltic ash, a variety of tuffs, reworked calcite-silica fragments, and both clear and colored pumice and dense glass fragments.

Organic control over the type of opal structure formed in the sand ramp environment can be seen in Fig. 22. This figure shows a cross section through a root cast; the wall of the cast contains numerous organic microstructures composed of dark brown opal-A, whereas the infilling formed after root death is of clear botryoidal opal-CT. This is evidence that organic materials can account for the formation of opal-A in sand ramps. The opal that formed by inorganic precipitation from solution or gel, however, is more ordered and forms opal-CT as in the infillings of dead plant cells in BB-3 (Fig. 21). As in the faults at Trench 14, opal-A is associated with organic structures and particularly with root sheaths.

V. SUMMARY AND CONCLUSIONS

Five types of analogs have been described for comparison with the calcite-silica deposits that occur within faults near Yucca Mountain. In making this comparison, it is important to bear in mind that the major depositional features in Trench 14 are abundant calcite and opal-CT, generally intergrown but with some relatively pure silica laminae. Clay minerals also occur, including smectites and chain-structure clays such as sepiolite. Opal-A is present where organic structures are preserved.

Hydrothermal veins from well-studied mineralized areas of the region are typically associated with sulfur-bearing minerals; some near-surface hydrothermal veins in the Calico Hills, closer to Yucca Mountain, do not contain sulfur but also lack calcite and contain a more ordered opal structure (opal-C) plus quartz and abundant manganese mineralization. No hydrothermal veins with the mineralogy of the Yucca Mountain fault fillings have been found.

Warm-spring deposits, whether in the active sinter-depositing systems of west-central Nevada, in the spring seeps of Oasis Valley, or in the fossil spring mound at Wahmonie, all contain abundant sulfur minerals. Opal can be found in some of the sinter deposits, but in all of the samples studied this is opal-A rather than opal-CT; other studies of sinter deposits suggest that the opal-A transforms to cristobalite, chalcedony, and quartz without going through an opal-CT stage. Calcite is rare. No warm-spring deposits with the mineralogy of the Yucca Mountain fault fillings have been found.

Cold-spring deposits of the region around Yucca Mountain are composed mostly of calcite. The weathering surface in the Moapa deposit that formed on the tufa outflow sheet tends toward smectite enrichment without opal formation. However, silica does occur as quartz in at least one spring mound along the

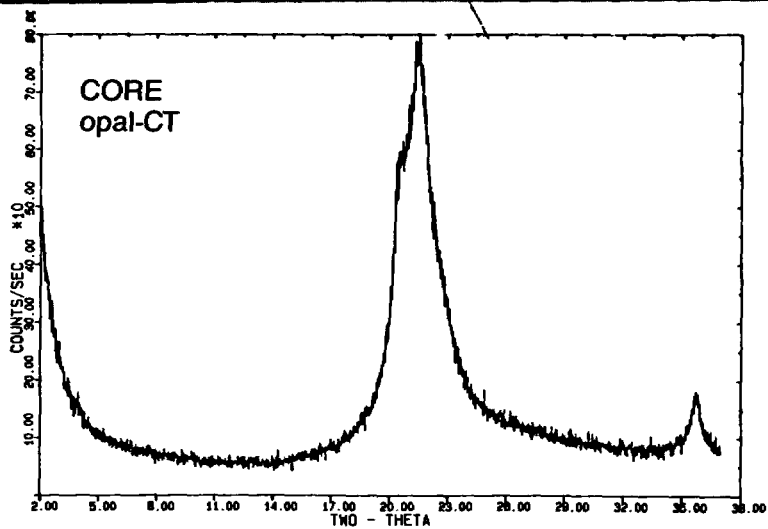
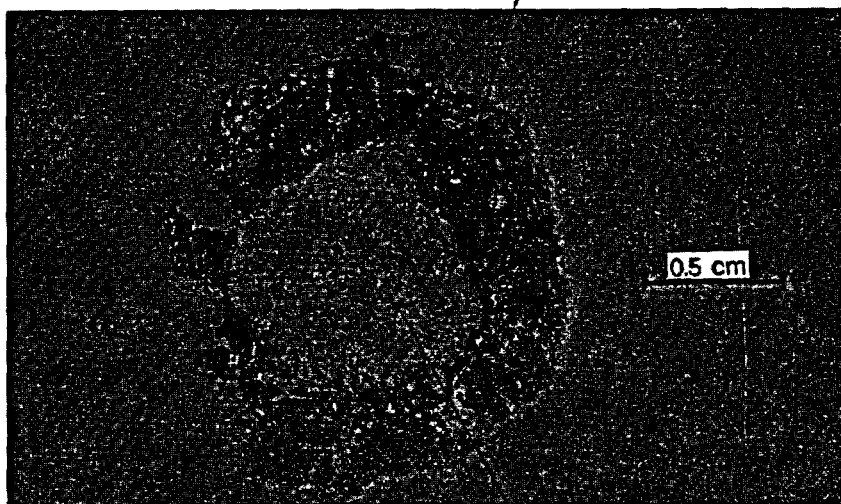
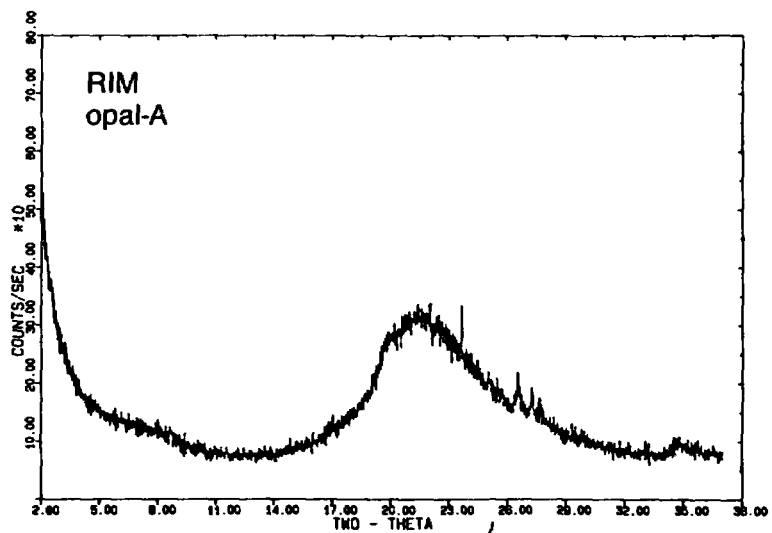


Fig. 22.
Photomicrograph of a fossil plant root (Larrea?) from the sand ramp along Fran Ridge near Trench 16. The cast formed by the living root is made of opal-A; infilling of the cast after plant death is of opal-CT.

Amargosa River and as opal-CT, chalcedony, and quartz along Carson Slough. Abundant sepiolite is intergrown with calcite (but without silica) in a seep along the eastern foot of the Eleana Range. All components of the Yucca Mountain fault fillings can be found in either cold-spring or seep deposits. However, the textures that result from flowing discharge (e.g., calcite tubules) and the remains of bull rushes are not found in the Yucca Mountain faults. Also, the restriction of silica deposition to late-stage replacement of carbonate in the playa/seep systems is different from the cyclic co-precipitation of calcite and opal in the faults around Yucca Mountain. Nevertheless, the partial similarity between fault and seep deposits suggests that further comparisons are needed.

Soils of the region contain calcrete deposits that include calcite, opal-CT, opal-A, smectite, and chain-structure clays and are similar to the deposits in faults around Yucca Mountain. In all of the soils formed on alluvial deposits near the faults, however, opal is a relatively minor component.

Aeolian sands close to the fault deposits contain both slope-parallel and fault-filling deposits of calcite, opal-CT, and a complex series of clays. Most importantly, the textures and relative abundances of calcite and opal-CT within small faults cutting the aeolian sand ramps are very similar to those in the larger faults north of the sand ramps in Trench 14. The similarity in mineral abundances is illustrated in Fig. 23, where XRD patterns of bulk calcite-silica materials from the faults in Trenches 14 and 17 are compared with the slope-parallel deposits from the sand ramps flanking Fran Ridge and Busted Butte. Occurrences of opal-A in both environments can be related to organic materials, and in particular to root sheaths. The similarity in constituents and the almost identical structure of slope-parallel deposits related to fault-filling deposits argue that, of all the analogs examined, the deposits in the neighboring sand ramps are most similar. One of our preliminary conclusions is, therefore, that the slope-parallel and fault-filling deposits in the sand ramps are closely related to the deposits exposed in Trenches 14 and 17.

The relationship between the very small sand-ramp fault deposits and the much larger fault deposits in Trench 14 and in Trench 17 is not trivial. If the similarity means that both were formed by the same process, the ability to examine that process operating on various scales and in different situations (both with and without a large underlying aeolian deposit) should help in constraining the process. For example, Fig. 19 shows a small fault that cuts the weakly consolidated sands along the western flank of Busted Butte. This

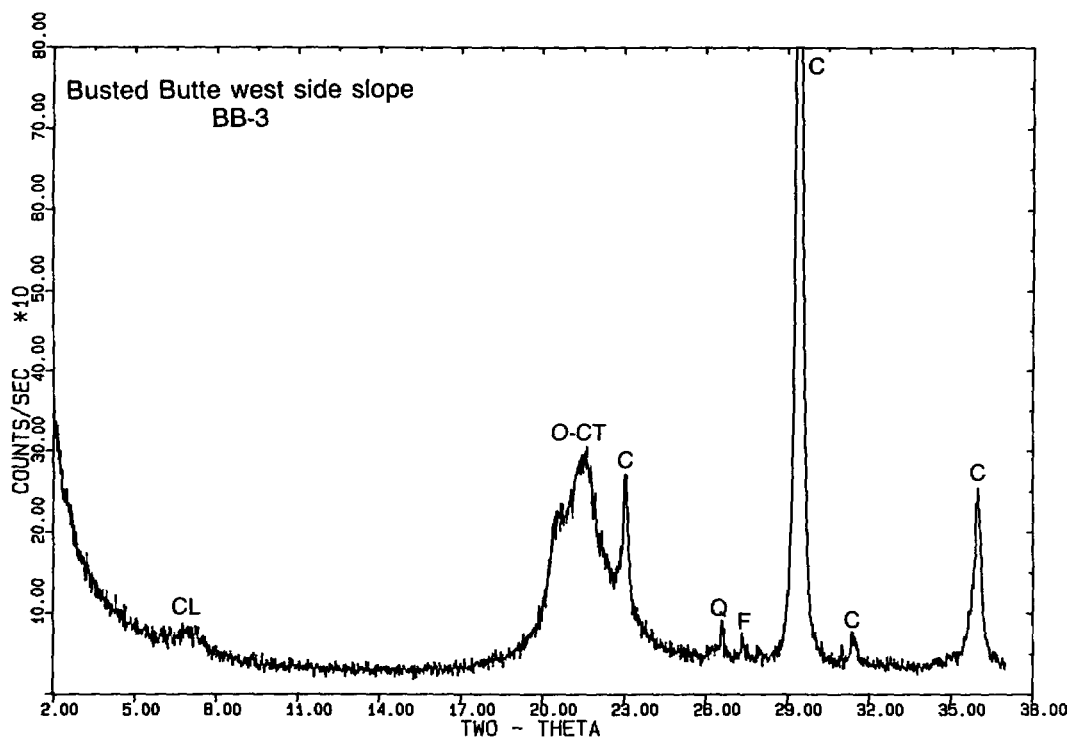
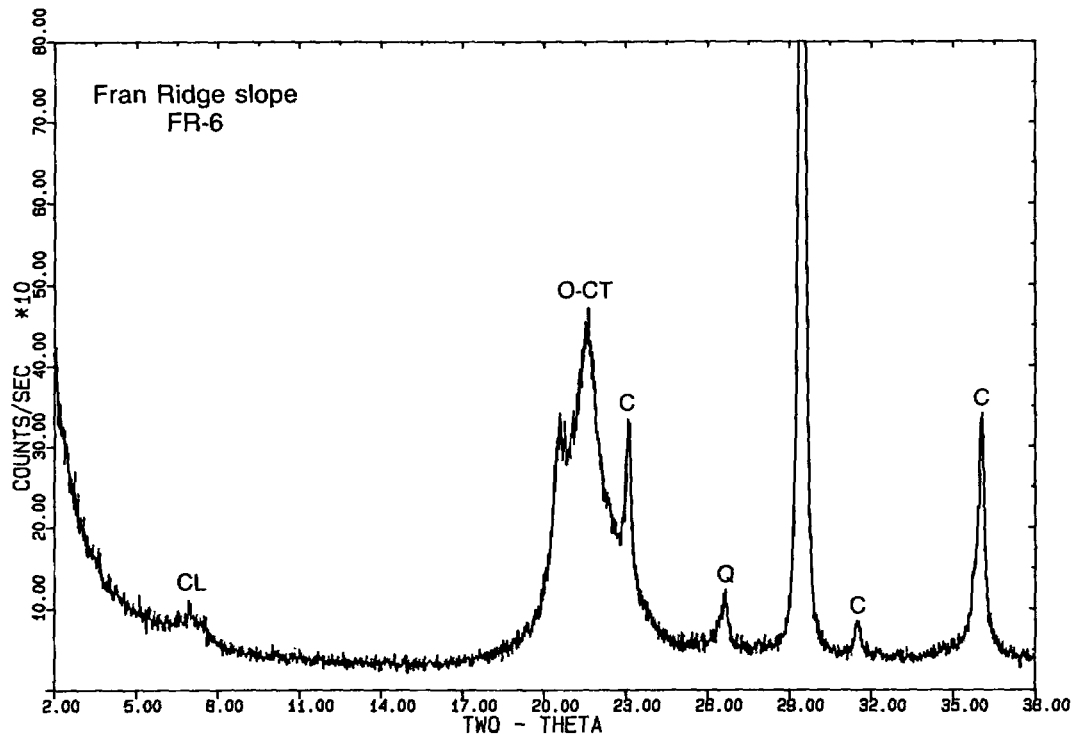


Fig. 23. Comparative XRD patterns for slope-parallel sand ramp deposits (FR-6 and BB-3) and deposits from trenched faults (T-14 brown and TR-17) along the eastern flank of Yucca Mountain. The subequal abundances of calcite and opal-CT are characteristic of both depositional environments.

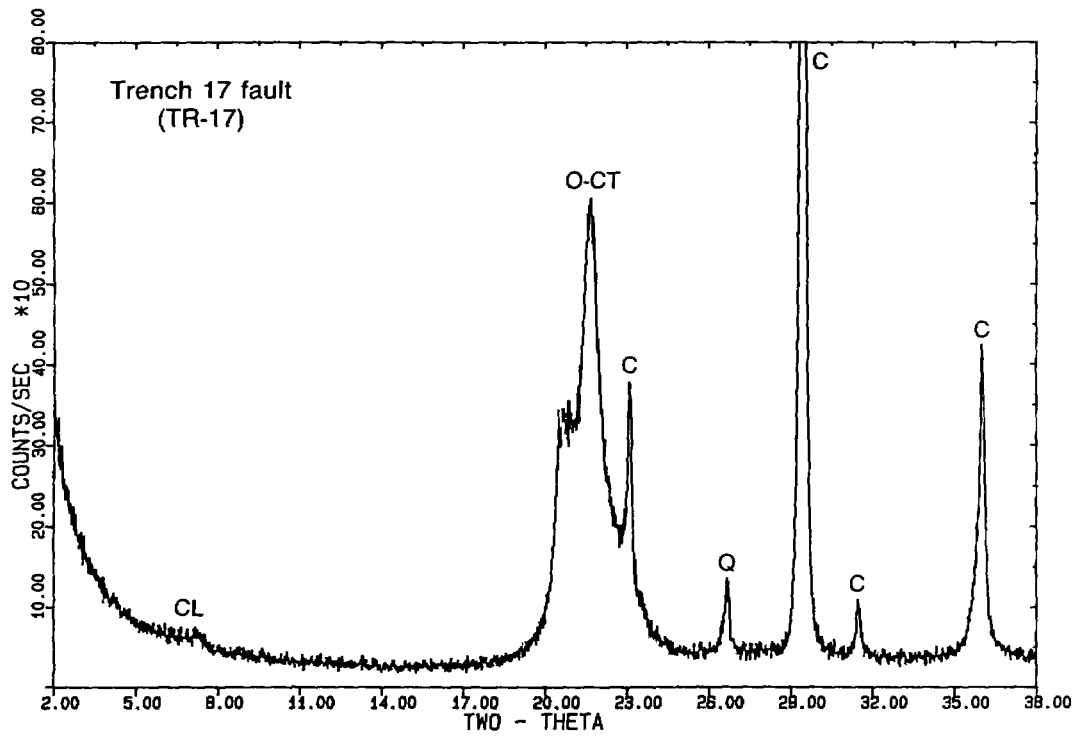
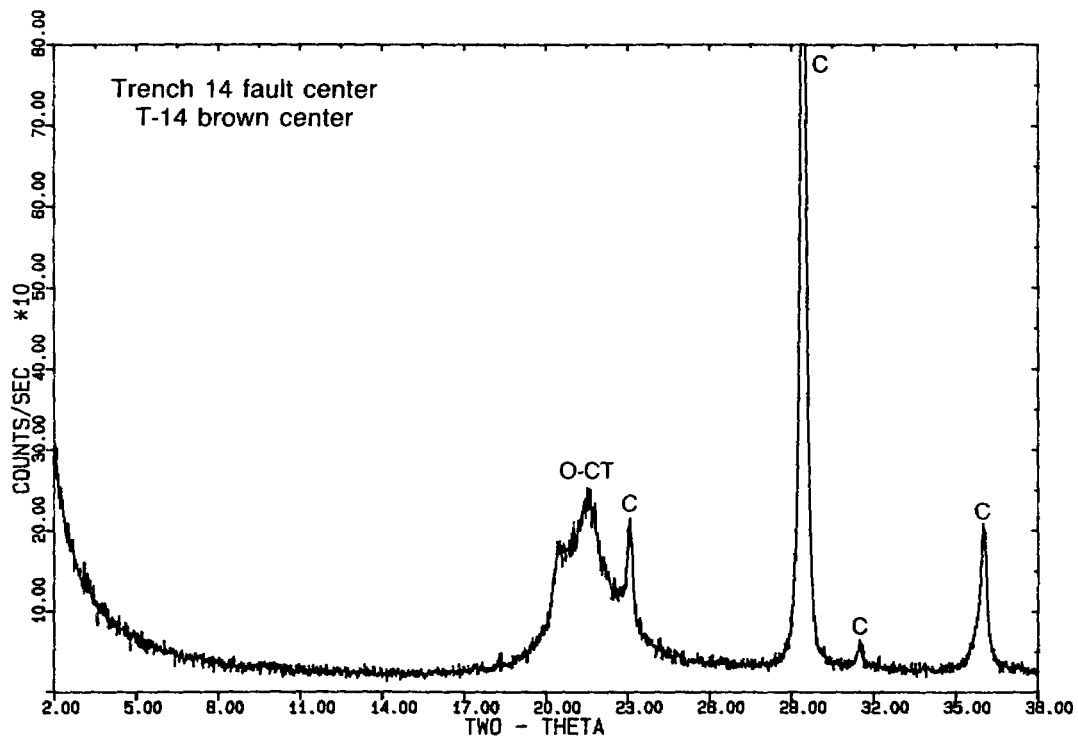


Fig. 23. (cont)

fault is visible because of the thin fault-filling deposit. At the bottom, the fault-filling deposit is a few millimeters wide and clogged with detrital grains. In this situation it would be unlikely that the materials deposited along the fault came from depth and rose upward under hydrologic pressure, confined within a very narrow fracture cutting poorly consolidated sand. In at least this occurrence transport downward seems much more likely. This exposure provides evidence that at least some fault deposits of this type did not originate by upward transport from depth. This conclusion is similar to that reached by Taylor and Huckins (1986) based on the mapping of Trench 14. However, the comparison of mineralogy presented in this paper is preliminary. Further studies of these deposits and of potentially analogous hydrothermal, warm-spring, cold-spring, and soil localities are planned in order to test these preliminary conclusions.

ACKNOWLEDGMENTS

The authors appreciate reviews by Grant Heiken, Schon Levy, and Steve Mattson. Discussions with John Hawley, Heather Huckins, John Stuckless, Jerry Szymanski, Emily Taylor, Don White, and John Whitney are reflected in this report. We are grateful to Barbara Hahn for help in report preparation, to Anthony Garcia for drafting, and to Marjorie Wilson for editing.

REFERENCES

- Bell, E. J., and L. T. Larson, "Overview of Energy and Mineral Resources for the Nevada Nuclear Waste Storage Investigations, Nevada Test Site, Nye County, Nevada," Nevada Operations Office report NV0-250, US Department of Energy (1982).
- Berger, B. R., and P. I. Eimon, "Conceptual Models of Epithermal Precious Metal Deposits," in Cameron Volume on Unconventional Mineral Deposits, W. C. Shanks, III, Ed. (Society of Mining Engineers of the American Institute of Mining, Metallurgical, and Petroleum Engineers, Inc., New York, 1983), pp. 191-205.
- Bish, D. L., "Detailed Mineralogical Characterization of the Bullfrog and Tram Members in USW-G1, with Emphasis on Clay Mineralogy," Los Alamos National Laboratory report LA-9021-MS (October 1981).
- Bish, D. L., "Evaluation of Past and Future Alterations in Tuff at Yucca Mountain, Nevada, Based on the Clay Mineralogy of Drill Cores USW G-1, G-2, and G-3," Los Alamos National Laboratory report LA-10667-MS (in preparation).

- Caporuscio, F., D. Vaniman, D. Bish, D. Broxton, B. Arney, G. Heiken, F. Byers, R. Gooley, and E. Semarge, "Petrologic Studies of Drill Cores USW-G2 and UE25b-1H, Yucca Mountain, Nevada," Los Alamos National Laboratory report LA-9255-MS (July 1982).
- Chadwick, O. A., and D. M. Hendricks, "Silica and Calcium Carbonate Interactions in Durargids," American Society of Agronomy 77th Annual Meeting (abstract), p. 189 (1985).
- Garside, L. J., and J. H. Schilling, "Thermal Waters of Nevada," Nevada Bureau of Mines and Geology Bulletin 91 (1979).
- Hay, R. L., and B. Wiggins, "Pellets, Ooids, Sepiolite and Silica in Three Calcretes of the Southwestern United States," *Sedimentology* 27, 559-576 (1980).
- Hay, R. L., R. E. Pexton, T. T. Teague, and T. K. Kyser, "Spring-Related Carbonate Rocks, Mg Clays, and Associated Minerals in Pliocene Deposits of the Amargosa Desert, Nevada and California," *Geological Society of America Bulletin* 97, 1488-1503 (1986).
- Hoover, D. L., W. C. Swadley, and A. J. Gordon, "Correlation Characteristics of Surficial Deposits with a Description of Surficial Stratigraphy in the Nevada Test Site Region," US Geological Survey open-file report 81-512 (1981).
- Horton, R. C., "Hot Springs, Sinter Deposits, and Volcanic Cinder Cones in Nevada," Nevada Bureau of Mines Map 25 (1964).
- Imai, N., and R. Otsuka, "Sepiolite and Palygorskite in Japan," in Palygorskite - Sepiolite: Occurrences, Genesis and Uses, *Developments in Sedimentology* 37 (Elsevier, New York, 1984), pp. 211-232.
- Jackson, M. L., "Soil Chemical Analysis - Advanced Course," published by the author, Madison, Wisconsin (1969).
- Jones, B. F., "Occurrence of Clay Minerals in Surficial Deposits of Southwestern Nevada," C. N. R. S. Colloquium on Petrology of Weathering and Soils, Paris (1983).
- Jones, J. B., and E. R. Segnit, "The Nature of Opal, I. Nomenclature and Constituent Phases," *Journal of the Geological Society of Australia* 18, 57-68 (1971).
- Kano, K., "Ordering of Opal-CT in Diagenesis," *Geochemical Journal* 17, 87-93 (1983).
- Kastner, M., J. B. Keene, and J. M. Gieskes, "Diagenesis of Siliceous Oozes - I. Chemical Controls on the Rate of Opal-A to Opal-CT Transformation - An Experimental Study," *Geochimica et Cosmochimica Acta* 41, 1041-1059 (1977).
- Khoury, H. N., D. D. Eberl, and B. F. Jones, "Origin of Magnesium Clays from the Amargosa Desert, Nevada," *Clays and Clay Minerals* 30, 327-336 (1982).

- LeConte, J., "On Mineral Vein Formation Now in Progress at Steamboat Springs Compared with the Same at Sulphur Bank," *American Journal of Science* **25**, 424-428 (1883).
- Milliman, J. D., Marine Carbonates; Recent Sedimentary Carbonates (Part I) (Springer-Verlag, New York, 1974).
- Montazer, P., and W. E. Wilson, "Conceptual Hydrologic Model of Flow in the Unsaturated Zone, Yucca Mountain, Nevada," US Geological Survey Water-Resources Investigations Report 84-4345 (1984).
- Oehler, J. H., "Hydrothermal Crystallization of Silica Gel," *Geological Society of America Bulletin* **87**, 1143-1152 (1976).
- Papke, K. G., "A Sepiolite-Rich Deposit in Southern Nevada," *Clays and Clay Minerals* **20**, 211-215 (1972).
- Post, J. L., "Sepiolite Deposits of the Las Vegas, Nevada, Area," *Clays and Clay Minerals* **26**, 58-64 (1978).
- Ross, H. P., D. L. Nielson, and J. N. Moore, "Roosevelt Hot Springs Geothermal System, Utah - Case Study," *American Association of Petroleum Geologists Bulletin* **66**, 879-902 (1982).
- Sawkins, F. J., Metal Deposits in Relation to Plate Tectonics, Series in Minerals and Rocks, No. 17 (Springer-Verlag, New York, 1984).
- Summerfield, M. A., "Silcrete," in Chemical Sediments and Geomorphology: Precipitates and Residua in the Near-Surface Environment, A. S. Goudie and K. Pye, Eds. (Academic Press, New York, 1983), pp. 59-91.
- Swadley, W. C., and D. L. Hoover, "Geology of Faults Exposed in Trenches in Crater Flat, Nye County, Nevada," US Geological Survey open-file report 83-608 (1983).
- Szabo, B. J., W. J. Carr, and W. C. Gottschall, "Uranium-Thorium Dating of Quaternary Carbonate Accumulations in the Nevada Test Site Region, Southern Nevada," US Geological Survey open-file report 81-119 (1981).
- Szabo, B. J., and P. A. O'Malley, "Uranium-Series Dating of Secondary Carbonate and Silica Precipitates Relating to Fault Movements in the Nevada Test Site Region and of Caliche and Travertine Samples from the Amargosa Desert," US Geological Survey open-file report 85-47 (1985).
- Taylor, E. M., and H. E. Huckins, "Carbonate and Opaline Silica Fault-Filling on the Bow Ridge Fault, Yucca Mountain, Nevada - Deposition from Pedogenic Processes or Upwelling Groundwater?" (abstract) *Geological Society of America Abstracts with Programs*, Flagstaff, Arizona, Meeting, **18**, p. 418 (1986).

- U. S. DOE, Environmental Assessment, Yucca Mountain Site, Nevada Research and Development Area, Nevada, Vol. I (US Department of Energy, Washington DC, 1986).
- White, A. F., "Geochemistry of Ground Water Associated with Tuffaceous Rocks, Oasis Valley, Nevada," US Geological Survey Professional Paper 712-E (1979).
- Williams, L. A., G. A. Parks, and D. A. Crerar, "Silica Diagenesis, I. Solubility Controls," *Journal of Sedimentary Petrology* 55, 301-311 (1985).
- Winograd, I. J., B. J. Szabo, T. B. Coplen, A. C. Riggs, and P. T. Kolesar, "Two-Million-Year Record of Deuterium Depletion in Great Basin Ground Waters," *Science* 227, 519-522 (1985).

Printed in the United States of America
Available from
National Technical Information Service
US Department of Commerce
5285 Port Royal Road
Springfield, VA 22161

Microfiche (A01)

NTIS		NTIS		NTIS		NTIS	
Page Range	Price Code						
001-025	A02	151-175	A08	301-325	A14	451-475	A20
026-050	A03	176-200	A09	326-350	A15	476-500	A21
051-075	A04	201-225	A10	351-375	A16	501-525	A22
076-100	A05	226-250	A11	376-400	A17	526-550	A23
101-125	A06	251-275	A12	401-425	A18	551-575	A24
126-150	A07	276-300	A13	426-450	A19	576-600	A25
						601-up*	A99

*Contact NTIS for a price quote.

